Received: 12 December 2019 | Revised: 13 September 2020 | Accepted: 28 October 2020

IET Renewable Power Generation

DOI: 10.1049/rpg2.12060

The Institution of Engineering and Technology WILEY

REVIEW

Layout optimisation algorithms and reliability assessment of wind farm for microgrid integration: A comprehensive review

Sachin Kumar[1] | R.K. Saket[1] | Dharmendra Kumar Dheer[2] | P. Sanjeevikumar[3] | Jens Bo Holm-Nielsen[3] | Frede Blaabjerg[4]

[1] Electrical Engineering Department, Indian Institute of Technology (Banaras Hindu University), Varanasi, Uttar Pradesh 221005, INDIA

[2] Electrical Engineering Department, National Institute of Technology, Patna, Bihar 800005, INDIA

[3] Center for Bioenergy and Green Engineering, Department of Energy Technology, Aalborg University, Aalborg, DENMARK

[4] Center for Reliable Power Electronics, Department of Energy Technology, Aalborg University, Aalborg, DENMARK

Correspondence
R.K. Saket, Electrical Engineering department, Indian Institute of Technology (Banaras Hindu University) Varanasi, Uttar Pradesh, INDIA.
Email: rksaket.eee@iitbhu.ac.in

Abstract

The paper represents a comprehensive review of the wind farm layout and reliability assessment of the wind farm integrated electrical power system. The authors have done a review on the proliferation of renewable energy which raises the uncertainties in the electrical power system. The uncertainties including wind speed and wake effect are important to deal with when an isolated microgrid is considered. The scenario becomes vigilant when the wind farms are integrated with the main grid. Due to uncertainties, the study of reliability evaluation of a wind integrated power system would become significant to analyse the electrical power system behaviour effectively. So, the paper discusses the layout optimisation methods of wind turbines considering the uncertainty parameters, mainly the wake effect. In this regard, the different wake models and optimisation methods based on a single-objective and multi-objective functions are reviewed in detail with the proper comparisons. The paper serves as a better illustration of the competency of these optimisation methods on the optimal wind turbine location on a wind farm. Furthermore, the paper extends the view on the reliability and cost assessment, and reliability improvement techniques of the wind integrated power system. This article provides comprehensive information, yields an attractive and subsequent tool for research requirements for the researchers to design the wind farm layout, and assessed the reliability of a wind integrated power system.

1 | INTRODUCTION

It becomes mandatory to fulfil the high-power demands, the renewable energy sources are integrated with conventional Electrical Power System (EPS) and/or work as the isolated microgrid spinning reserves [1]. The Off-shore renewable energy systems are fully developed technology among all renewable sources, which is further beneficial when incorporated with the commercial market [2]. So, to achieve the high demands, the incremental sizing parameters including rotor diameter, rated power, and a hub height of wind turbines (WTs) are required, which also decreases the running and initial costs of the Wind Farm (WF) [3]. Thus, the cost needs to be minimised with a higher output power of the WT to meet the demand without affecting the system's reliability. Moreover, Table 1 illustrates that many researchers have concentrated their work on WT optimal location. Thereby, it is desirable to

Abbreviations: AAA, Artificial Algae Algorithm; AC, Alternating Current; ACO, Ant Colony Optimization; AEP, Annual Energy Production; AOH, Annual Outage Hour; CFD, Computational Fluid Dynamics; DC, Direct Current; DE, Differential Evolution; DFIG, Doubly-Fed Induction Generator; DSM, Demand Side Management; EAF, Equivalent Availability Factor; EENS, Expected Energy Not Supplied; ENS, Energy Not Supplied; EPDS, Electrical Power Distribution System; EPS, Electrical Power System; EV, Electric Vehicle; GA, Genetic Algorithm; GH, Garrad Hassan; GR, Generation Ratio; GRA, Generation Rescheduling Algorithm; GSC, Grid Side Converter; HAWT, Horizontal Axis Wind Turbine; IEEE, Institute of Electrical and Electronics Engineers; kWh, Kilowatt Hour; LES, Large Eddy Simulation; LOEE, Loss of Energy Expectation; LOLE, Loss of Load Expectation; LOLP, Loss of Load Probability; LPC, Levelized Production Cost; MCS, Monte-Carlo Simulation; MOGOMEA, Multi-Objective Gene-pool Optimal Mixing Evolutionary Algorithm; MOWFLOP, Multi-Objective Wind Farm Layout Optimization Problem; MV, Megavolt; NPV, Net Present Value; OM, Operation and Maintenance; OSS, Offshore Electrical System; OWF, Off-shore Wind Farm; PDF, Probability Density Function; PL, Parking Lot; PSOParticle Swarm Optimization, PV; Photo Voltaic, RAM; Reliability Availability Maintainability, RANS; Reynolds-Averaged Navier-Stokes, RBTS; Roy Billinton Test System, RTS; Reliability Test Network, SAIDISystem Average Interruption Duration Index; UPF, Unity Power Factor; V - G, Vehicle to Grid; V - H, Vehicle to Home; V AWT, Vertical Axis Wind Turbine; viz, which is; V SC, Voltage Source Converter; WF, Wind Farm; WIPS, Wind Integrated Power System; WT, Wind Turbine; WTG, Wind Turbine Generator

TABLE 1 Illustration of previous research works

S. No.	Research work	Method(s) used	Remark(s)	Reference
1.	To obtain the optimised locations of WTs in a WF	New mathematical framework, Binary Artificial Algae Algorithm (AAA), algorithms of 'Genetic and evolutionary computation conference' 2015, NSGA-II, strength Pareto evolutionary algo2, and indicator-based evolutionary algorithm, Spatial decision support system	The factors such as hub heights, number of WTs are considered and exact wake effect structure is formulated and compared with previous works. The evolutionary algorithms are studied and implemented to get optimised WF layout with 10, 20, 30, etc., WTs.	[20–23]
2.	WT placement along with Jensen's linearity model of wake in order to obtain the optimal WT location of a given dimension WF	New pseudo-random number generation, Non-linear mathematical (NLM) model, Enhanced GA, Particle Swarm Optimisation (PSO)	Wake effect is considered and obtained results are compared with previous works based on Gas, viral basis methods, etc.	[24–29]
3.	To assess the wind energy potential under uncertainties	MCS, Geographic Information System (GIS), Piece-wise linear mixed-integer optimisation using General Algebraic Modelling System (GAMS), MCS, Quadratic interpolation, Genetic Algorithm (GA)	Data of weather forecasts is analysed, MCS is used in wind field and energy production simulations. Cost and reliability are major concerns.	[30–33]
4.	To get the optimised trade-offs between capital investment, energy production, and operational costs in OWFs	Multi-objective Gene-pool optimal mixing evolutionary algorithm	MOGOMEA outperforms the NSGA-II when applied to solve the MOWFLOP	[34]
5.	To analyse the cost and efficiency of OWF	Geometric program	The physical layout and configuration are determined for AC and DC systems	[35]
6.	To improve the power production and reduce the cable cost and length	Ant Colony Optimisation-Multiple travelling salesman problem (ACO-MTSP)	The goals are achieved by considering WT location, substation location, submarine cables, and cable length.	[36]

consider the maximum power under wake effects and other uncertain parameters at minimum cost and minimum land area. The consideration of uncertainty is too important to analyse due to the fact that the output power and overall cost must be optimal. The output power and overall cost are the functions of uncertain parameters.

In EPS, it is a prerequisite to deal with the uncertain parameters of sustainable energy sources. 'Uncertainty', which contributes to the unreliability of the system, involves possibilistic [4–6] and probabilistic [7–9] handling procedures. In the possibilistic method, fuzzy membership functions are employed to illustrate the uncertain parameters and it is determined with fuzzy arithmetic. In the probabilistic method, the design of uncertain parameters is performed by Probability Density Functions (PDFs) and later evaluated with the programs including Monte-Carlo Simulation (MCS) [10] and Point Estimate Method (PEM) [11].

Thus, the paper considers the wind effects on the rear side of WTs by demonstrating the different wake models developed by Jensen, Larsen, Lissaman, etc. To study the effect of wind direction, a Wind Rose diagram is also described. This paper also overviews the WT-driven IG (known as WECS) for renewable energy applications [12–14]. The description of wake effect models leads to obtaining the optimal WT locations in a WF. An optimal WF layout configuration is described by explaining some optimisation techniques. The motive of an optimal WF layout is to maximise the annual energy production (AEP) at a minimum cost per total power. The detailed description on AEP is given in [15, 16]. To achieve this objective, researchers in [17, 18] have described and discussed the techniques for optimal deployment of wind turbine generators in WFs. The applications of various optimisation techniques including Pseudo number random generation and binary artificial algae algorithm (BAAA) are discussed and explained mathematically. Further, the reliability and economical models are considered in the WF design assessment, and reliability assessment with its improvement methods are also discussed for WF-integrated EPS [19].

To accomplish the above discussions, the paper has demonstrated theoretically and mathematically about different optimisation techniques and algorithms. In this regard, the paper is organised into six sections. Section 2 describes the uncertainty models which are incorporated for study. In Section 3, the implementation of uncertainty models in obtaining the optimised WF layout is mentioned. The reliability and cost analyses considering the uncertainties in optimising the WT location and WT failures are discussed in Section 4. The reliability improvement techniques are presented in Section 5. Conclusions with the scope of future work are presented in Section 6.

The researchers of the WF layout optimisation field and its reliability have shown tremendous interest. The workflow of this paper is shown in Figure 1 which is delineated the prime contributions of this review paper as follows.

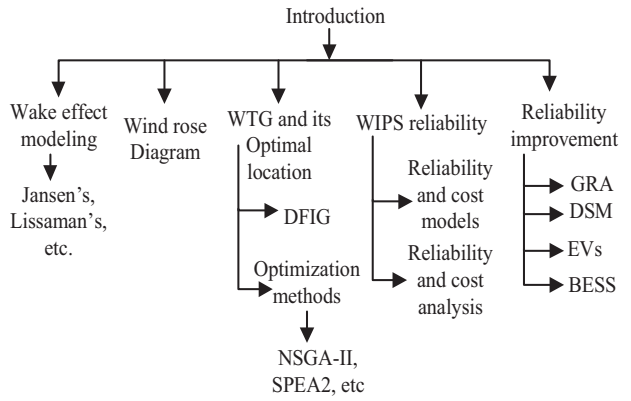

FIGURE 1 Work flow of research paper

i. The study of WT location optimisation under uncertainty.
ii. Consideration of reliability aspects.
iii. Discussion on different optimisation methods.
iv. The reliability improvement methods are discussed when WF is integrated with power systems such as Roy Billinton Test System (RBTS), and IEEE Reliability Test Network (RTS).

2 | WAKE EFFECT MODEL, WIND ROSE DIAGRAM AND PROBABILISTIC APPROACH

As per the capacity and size of WF, the type of WT (Horizontal Axis Wind Turbine (HAWT) and Vertical Axis Wind Turbine (VAWT)) is chosen. Further, it is inspected that for large WFs, HAWT is generally used whose rotational axis is parallel to ground. The number of WTs allocated depends on the size of WF. Due to such allocations of Wind Turbine Generators (WTGs), there is a wake effect established for the downstream WTs. Firstly, WT extricates energy from wind and then creates turbulence carried to the downstream which reduces the power production of the WTs. In particular with low-frequency meandering, intermittent edge, velocity deficit, and shear layer generated turbulence. Hence, it becomes necessary to develop a wake effect model to achieve maximum power with optimised Off-shore Wind Farm (OWF) planning. To analyse the wake effects, some software including Wind Atlas Analysis and Application Program, WindPRO, WF for simple modelling, and Computational Fluid Dynamics (CFD) model from ANalysis SYStems for full modeling are available. The wake models' ranking with their inputs for the mathematical models are mentioned in Tables 2 and 3, respectively. So, this section describes various wake models that are developed and used for WT layout optimisation.

2.1 | Wake models

Various wake models available in literature are explained in this subsection.

TABLE 2 Wake models and their hierarchy

Type	Wake model
Empirical	Jensen (1983) or Katic (1986) (useful in power production and AEP reliability analysis)
Linearised RANS	Eddy-Viscosity Fuga (useful in power production and AEP reliability analysis)
Other	Dynamic wake meandering Stochastic
Nonlinear RANS	k-ω closure with actuator disk, line
Large Eddy Simulation (LES)	Dynamic Smagorinsky with actuator disk, line

TABLE 3 Input parameters in different wake models

Inputs	Jansen's	Frandsen's	Larsen's
Intensity of turbulence			Yes
Height of hub			Yes
Diameter of rotor	Yes	Yes	Yes
Distance from the WT (radially)			Yes
Downstream distance from the WT	Yes	Yes	Yes
Inflow wind speed	Yes	Yes	Yes

2.1.1 | Jensen's model

This model is developed mathematically by Jensen [37] and further, Katic [38] modified the model by assuming that the wake zone is circular cylindrical. The linear expansion of wake with downstream distances are increased, and the cross-sectional wake velocity is uniform at all points; viz top-hat likes distribution as shown in Figure 2(a). The model is derived by considering the wake's momentum balance and wake velocity is found as given in (1), on which the output power of a downstream WT is dependent.

$$V_d = V\left[1 - \frac{2a_f}{\left(2\alpha_d \frac{Z}{D_u}\right)}\right], \tag{1}$$

where V is the inflow speed of wind, V_u is the velocity behind the WT rotor, V_d referred as velocity under wake effect at a distance 'Z' from the front rotor, D_u is rotor diameter, D_d is wake diameter at distance 'Z', Z_H hub height of the front rotor, α_d is a decay coefficient (constant), and α_f is an axial induction factor.

The velocity deficit at point 'Z' is given in (2)

$$1 - \frac{V_d}{V} = \frac{1 - \sqrt{1 - C_\tau}}{\left(1 + 2\alpha_d \frac{Z}{D_u}\right)^2}, \tag{2}$$

where C_τ is known as thrust coefficient.

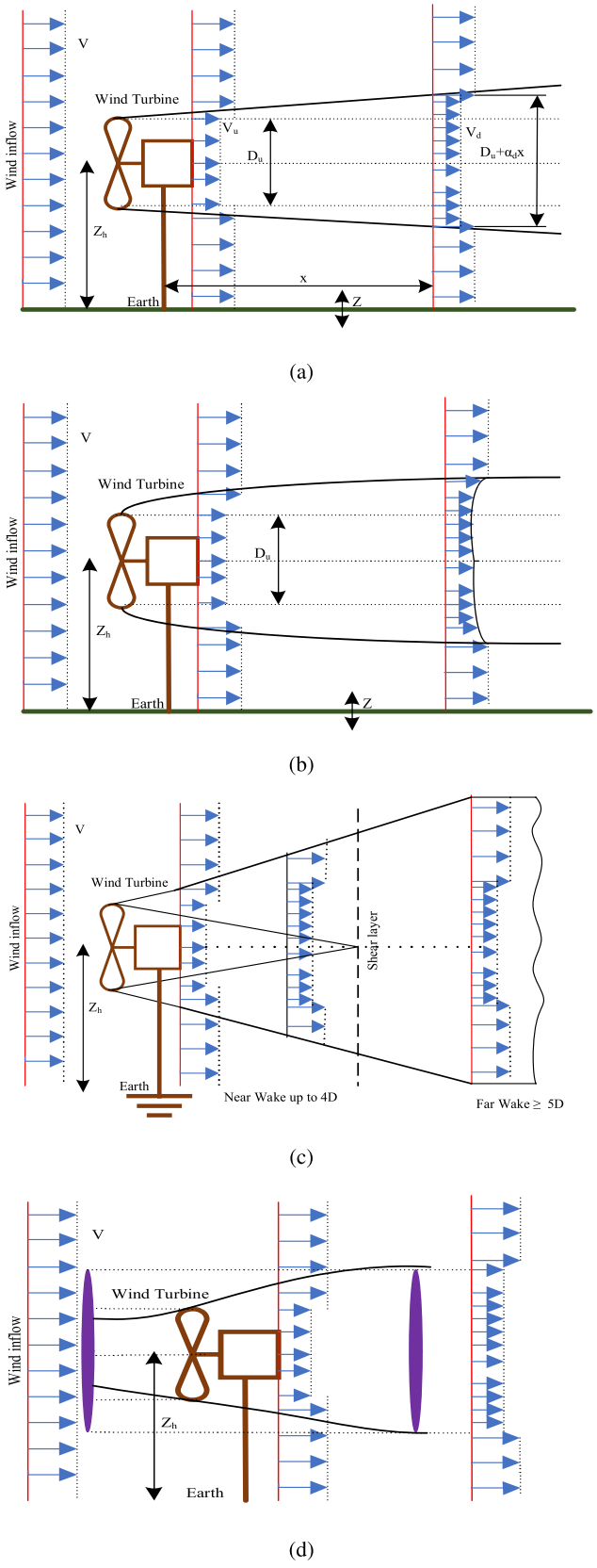

FIGURE 2 Different Wake models. (a) Jensen's wake model, (b) Larsen's wake model (c) Lissaman's wake model and (d) Frandsen's wake model

2.1.2 | Larsen's wake model

In this model, it is modified that wake behind the rotor is not linear but has some perturbation on average wind flow. It is due to the normal shear and wakes itself. This model is developed by Larsen [39], referred to as '1988 Early version' [40]. The early version considers only the single wake and is not suitable for multiple wake effects. This model proposes a version that describes the boundary conditions with a proper WF approach by using an analysis of experimental results and this version is termed as '2009 Later version' [41]. As per the model shown in Figure 2(b), the velocity deficit, wake radius for boundary condition at the plane of the WT rotor, and wake radius at a fixed frame of reference placed at a distance $9.6D_u$ are given by (3)–(5), respectively.

$$\Delta U(s', r') = \Delta U^1(s', r') + \Delta U^2(s', r'), \tag{3}$$

$$R_{\text{wake}} = \left(\frac{105a_1}{2\pi}\right)^{\frac{1}{5}} C_\tau A(\chi + \chi_0)^{\frac{1}{3}}, \tag{4}$$

$$R_{9.6D_u} = c_1(e^{c_2 - c_\tau^2 + c_3 C_\tau + c_4})(d_1 i_a + 1)D_u. \tag{5}$$

The velocity deficit is the function of (s', r') where (s', r') is the distance and radial coordinates, ΔU^1 and ΔU^2 are the first- and second-order contribution to the velocity deficit ΔU, 'A' is the WT rotor swept area and initial distance Z_0 is given by (6).

$$Z_0 = \frac{9.6D_u}{\left(\frac{2R_{9.6}}{KD_u}\right)^3 - 1}, \tag{6}$$

where a_1 is a coefficient given by $(\frac{KD_u}{2})^{\frac{5}{2}}(\frac{105}{2\pi})^{-\frac{1}{2}}(C_\tau A Z_0)^{-\frac{5}{6}}$, where $K = \sqrt{\frac{M+1}{2}}$, and $M = \frac{1}{\sqrt{1-C_\tau}}$, i_a is the intensity of ambient turbulence, c_1, c_2, c_3, c_4, d_1 are coefficients and determined empirically.

2.1.3 | Lissaman model

This model [42] is developed by the use of momentum and blade element theories. Its modelling is based on fluid mechanics and dividing wake area into smaller areas as shown in Figure 2(c). However, due to these divisions, it is quite difficult to define the border between these areas or regions.

Further, a simpler and accurate model is developed and referred as Ainslie's wake model which uses the axial symmetric Reynold's and numerical solution of the Navier–Stokes for the turbulent boundary layers in wake modelling. However, due to its complicated numeric solutions, it may be restricted in the use commercial software such as GH WindFarmer.

2.1.4 | Infinite WF boundary layer model

This model is developed by Frandsen and hence, it is also referred to as Frandsen model [43]. It is fully based on the

conservation law of momentum of the wind flow through the WT rotor and rotor layer. The wind flow follows the logarithmic profile with a reduction as given in (11). Further, Frandsen has assumed that the shape of wind flow is cylindrical with a stable cross-sectional area which is equivalent to the wake area. The adapted model diagram is shown in Figure 2(d) and the mathematical modellings are described in (7) and (8).

$$D_{\text{wake}}(z) = D_u(\alpha^{\frac{K}{2}} + \alpha_d S)^{\frac{1}{K}}, \tag{7}$$

$$V_d = \frac{V}{2}\left(1 \pm \sqrt{1 - 2\frac{A}{A_w}C_\tau}\right), \tag{8}$$

where α is termed as wake expansion coefficient which is given by $\frac{1+\sqrt{1-C_\tau}}{2\sqrt{1-C_\tau}}$, relative distance from rotor is $S = \frac{Z}{D_u}$, $D_{\text{initial}} = \sqrt{\alpha}D_u$, '$K$' is a constant and determined empirically, and A_w is the wake area at distance 'Z'.

2.1.5 | Fuga

It is an engineering tool that uses Reynolds-Averaged Navier-Stokes (RANS) in linear form and builds downstream wind velocity using lookup tables. It is one of the powerful CFD-based models to develop single and multiple wake effect mathematical model as described in [44]. It does not require to model the wind inflow using a logarithmic profile with stable effects and the drag force terminology as mentioned in (9). It uses an actuator disk model containing layered control volume.

$$F_x = -\frac{1}{2}C_T {U_f}^2 \delta(x - x_h)\gamma(R^2 - (y - y_h)^2 - (z - z_h)^2). \tag{9}$$

The F_x is termed as drag force which is modelled by considering an actuator disk model with a layered control volume, where 'δ' is referred to as delta function and 'γ' is denoted as a step function which is 0 for −ve arguments and 1 for +ve arguments, 'z' is the elevating distance above ground level, 'z_h' is the height of wind.

2.1.6 | EllipSys3D

It is a three-dimensional CFD-based resolver with a block-structured finite volume approach [45] and may use a number of models related to turbulence. The two models namely RANS and LES versions are accessible in EllipSys3D model. In the RANS-based model, WT rotor is modelled as an actuator disk. The elliptical Navier–Stokes is developed with discretised non-linear terms in RANS- and LES-based models. The rotor is modelled as a line of actuator where the Boundary Element method defines the axial pressure or force and velocity profile is described by RANS and LES versions as given in (10) and (11).

RANS version of EllipSys3D represented numerically as

$$V_T = C\gamma F_P \frac{K^2}{\mu} \tag{10}$$

EllipSys3D can be represented as $K - \mu - F_P$ and $K - \mu$ models. In standard $K-\mu$ model, $F_P = 1$ and $C_\gamma F_P$ is a constant termed as an effective Eddy-viscosity coefficient. V_T = eddy viscosity, $C\gamma$ = a model constant, K = turbulence kinetic energy, μ = dissipation.

In $K - \mu - F_P$ model, F_P is a scalar function and depends on local parameter of shear, $\sigma_s = \frac{K}{\mu}\sqrt{(U_{i,j})^2}$ where σ_s is termed as shear parameter and $U_{i,j}$ is the velocity coordinates.

LES version of EllipSys3D:

$$U(z) = \frac{U^*}{K}\ln\left(\frac{Z}{Z_0}\right), \tag{11}$$

where $U(z)$ is the average speed of the wind, U^* refers to a frictional velocity, K denotes Von Karman constant, Z, and Z_0 are the elevation from the ground and roughness length from the surface, respectively.

2.2 | Wind rose diagram

It is a diagram that is developed by using a graphical tool. Meteorologists use this diagram to get a succinct perspective of speed and direction distribution of wind at a specific location. The diagram uses a polar coordinate system where the frequency of winds is plotted by wind direction over a time period. Previously, the wind rose is referred to as a compass rose and there was no difference between a principal direction and the wind approaching from such directions. The largest spike shows the direction of the wind with maximum frequency at a particular location. Thus, each spike length throughout the circle is associated with the frequency that the wind moves from a specific direction per unit time. The circles placed concentrically refers to different frequencies from origin to outer circle. Figure 3 shows coloured spokes that represent the wind speed ranges. It may be divided into 16 or 32 cardinal directions, such as north and north-north-east [46]. The angle is measured in degrees, such as North signifies 0° and 360°, East 90°, South 180°, and West 270°. The main implementation of this diagram is shown in wind farm design, airport runways, weather forecasts, etc.

2.3 | Probabilistic approach

This approach is implemented considering the uncertainties including wind and solar energy generation, battery charging and discharging, dynamics of an electric vehicle (EV), load variation, and electricity rate. The probabilistic methods including PEM and MCS are implemented after modelling the uncertain parameters into probability density function. The two important methods include PEM and MCS are described as follows.

FIGURE 3 Wind rose diagram [46]

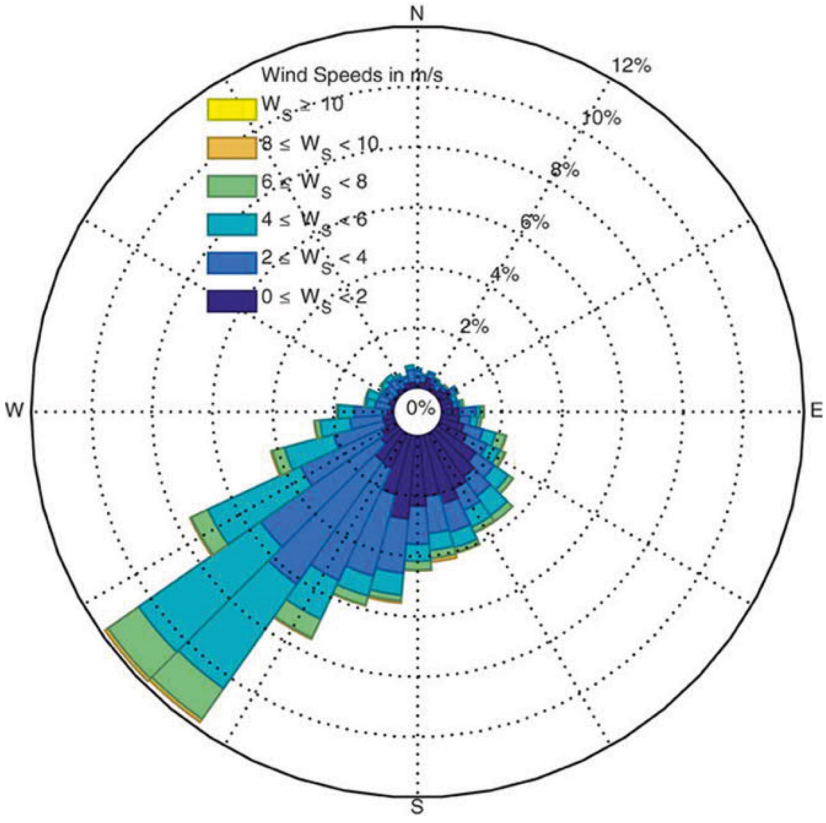

2.3.1 | Point estimate method

This method identifies a single value index such as mean, mode, and median, which serves as 'exact estimation' of an unspecified parameter from a random sample. Maximum likelihood estimator and method of moments are the general methods used for point estimation. Firstly, it is introduced [47] in the year of 1975 by Emilio Rosenblueth. The detailed qualitative description of point estimate methods can be obtained in [48]. The probabilistic uncertainties of the distributed generator, load, and ESS were considered in [49] and an operational risk assessment model based on PEM was proposed. An improved version of PEM namely 3PEM in [50] was proposed to evaluate the probability moments of probabilistic power flow. This method was developed using 3PEM, 2PEM, and Chebyshev inequality. Further, PEM was implemented in [51] to reduce the number of scenarios that model wind energy and load uncertainties. Thus, the PEM is a very strong tool for analysing the uncertain parameters.

2.3.2 | Monte-Carlo simulation method

A very large number of trials generate a good estimate of the probability and thus reliability. Therefore, a large number of trials are required through a random process. In spite of oscillations in probability, the MCS method leads to the true value as the number of trials is increased. MCS is implemented to obtain the probability of success and failure of the stochastic electrical power system. On the other side, the MCS method is used in estimating the reliability indices by actual simulation process and system's random behaviour. The MCS method, therefore, deals with the problem as a serial real experiment conducted in a stipulated time. This MCS method evaluates the probability and reliability indices by counting the occurrence of event numbers [52].

3 | WIND TURBINE GENERATOR AND ITS OPTIMAL LOCATION

The HAWT is advantageous over VAWT such as self-starting nature, clear siting due to tower height, maximum wind energy extraction even in rumble land, and adaptation to wind direction by adjusting nacelle and blade directions. The components like the gearbox, shaft, and generator in HAWT are placed at the top of the tower and transformer at the bottom. The WTG is one of the highlighted components in the WT because it is chosen to extricate maximum wind energy from the wind with variable speed. So, Subsection 3.1 discusses the types of WTGs with their benefits and applications, and few WF layout optimisation methods are briefly explained in subsequent subsections.

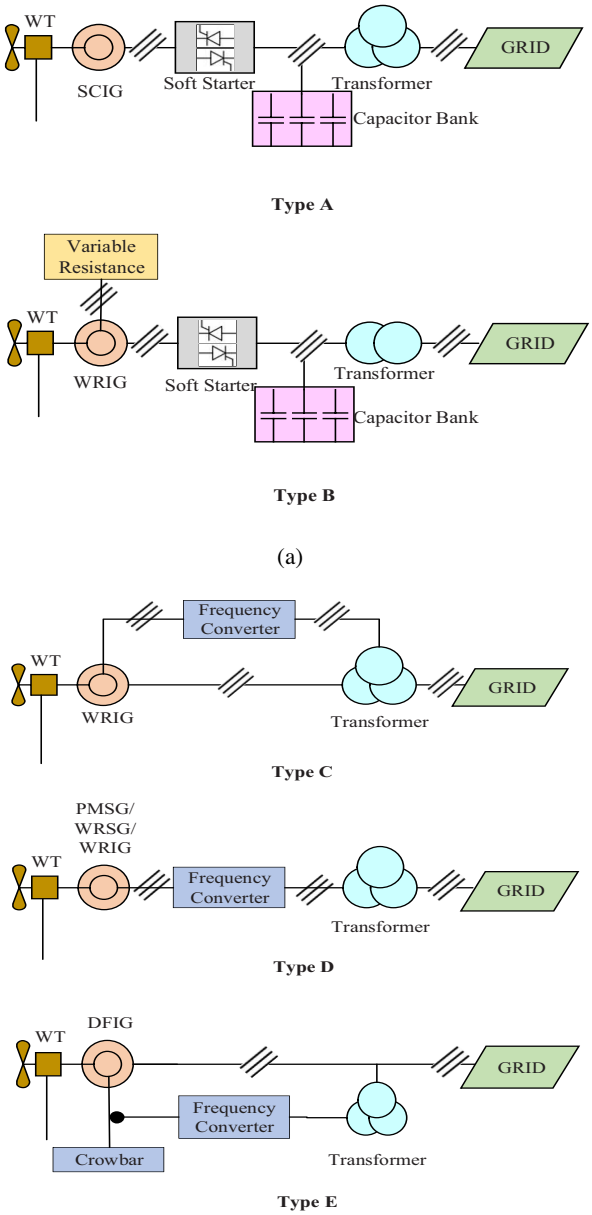

FIGURE 4 The five configurations Type A, B, C, D, E of induction and synchronous generators implemented with WT. (a) SCIG and WRIG configuration. (b) PMSG and DFIG configuration

3.1 | Wind turbine generator

The configurations of generators which are used for power generation with WTs are shown in Figure 4(a) and (b) of [53]. The asynchronous (induction) generator mainly Doubly-Fed Induction Generator (DFIG) which is generally implemented as WTG is explained in this subsection. The advantages of induction generators over synchronous generators are as follows.

i. 'Q' controlling is possible.

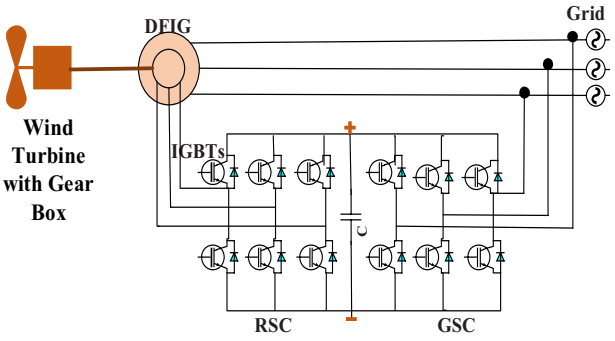

FIGURE 5 RSC and GSC in DFIG-based WECS

ii. Isolated 'P' and 'Q' controlling is possible by the excitation control of rotor independently.
iii. Magnetisation from the grid is not required as rotor circuit may magnetise the DFIG.
iv. It generates 'Q' and fed back to the stator by Grid Side Converter (GSC).

3.2 | Doubly-Fed Induction Generator

The stator voltage is exerted from the power grid and the rotor voltage is impelled by the power converter hence, referred to as doubly fed. The connection of the stator winding is direct to the invariable frequency grid and the winding of the rotor is placed to a bidirectional back-to-back Voltage Source Converter (VSC). It allows a large range of speed variations in a limited manner. This property is utilised in WTG where the WT rotor speed varies with volatility in wind speed. If the speed leads to an over-synchronous situation, the power flows from the rotor through VSC into the power grid. Whenever a sub-synchronous situation occurs, then the power flows in the opposite direction. The converter as shown in Figure 5 compensates the imbalance between the electrical and mechanical frequencies where Rotor Side Converter (RSC) manages the active power 'P' and reactive power 'Q' by controlling the rotor current, and GSC manages the DC-link voltage and confirms unity power factor operation. Thus, DFIG is a crucial part of the WT due to the above-mentioned advantages and characteristics and hence referred to as the WTG. To get the maximum power in a WF, the WTs locations are required to be known optimally with minimum land area and minimum overall WF cost. To accomplish the task, Subsection 3.2 discusses the methods for WTs' optimal locations considering wake effects and other uncertainties.

3.3 | Wind turbine location

WFs may be developed with 10, 20, 30, and more WTs to get the power output required by the utilities. The number of wind turbines must be placed such that the maximum energy would be extracted considering the wind speed variability. Researchers have solved the WT layout problem by using GA [25], simulated

TABLE 4 Insight on optimisation methods implemented in WF Layout

Classical methods	Non-classical methods	Stochastic programming techniques
(i) Linear programming, (ii) Mixed integer linear programming, (iii) Mixed integer nonlinear programming, (iv) Geometric programming, (v) Vertex packing algorithm	(i) Binary layout codification, (ii) Free layout optimisation, (a) Heuristic, (b) Metaheuristic, and (c) Hybrids	(i) Bender's decomposition, (ii) Dantzig-Wolfe, (iii) Stochastic dynamic programming (iv), Approximate dynamic programming

annealing [26], DE [27], ACO [28], PSO [54], definite point selection [55], and stochastic evolution [23]. Authors [24, 56, 57] have given the optimisation techniques for WF layout problem considering wake effects. Some of the important optimisation methods are discussed in this subsection and some of the optimisation methods are described in Table 4 which are used to obtain optimal WF layout.

3.3.1 | Strength Pareto Evolutionary Algorithm2

Several Evolutionary algorithms including SPEA2 (Strength Pareto Evolutionary Algorithm2) and NSGA-II (Non-Dominated Sorting Genetic Algorithm-II) are implemented for multi-objective problems. As these techniques produce the Pareto optimal solutions, thus implemented to obtain the optimal WT layout and the locations of the distributed generators in the system [58]. The two main objectives and two main issues are involved in SPEA Pareto-optimal set which are as follows:

Objective No. 1: Minimisation of optimal front distance

Objective No. 2: Maximisation of generated solutions

Issue 1: To supervise the search properly near the Pareto-optimal front.

Issue 2: To keep the individuals specifically during the evaluation process.

SPEA2 uses an external set (archived) and a regular population in which non-domination members are archived to replace any duplicate member and then the fitness values are designated to archived and population members. The algorithm steps to follow in SPEA2 are discussed below [33].

Step I: A strength value $S(p) \in [0, 1]$ is provided to the individual archives i and at this time it represents its fitness value $F(p)$. $S(p)$ is the number of population members q that is influenced by or equal to p with respect to the objective values, divided by population size plus one.

Step II: The summation of strength values of all the archived members p that dominates or equivalent to q is used in the calculation of fitness $F(q)$ of an individual ' in the population, and add one at last.

Step III: By using the binary tournaments, the selection of the mating phase in which individuals from the union of population and archived members are chosen. The minimisation of fitness is expected in this step, due to which archived individuals have a higher selection chance than any other population members.

Step IV: The older population is exchanged by the resulting offspring population when the mutation and recombination process is once over.

3.3.2 | Non-Dominated Sorting Genetic Algorithm-II

NSGA-II alleviates the computational complexity, non-elitism approach, and the need for specifying sharing parameters. This method is useful in achieving a good convergence and better spread of solutions when compared to Multiobjective Evolutionary Algorithms-Pareto Archive Evolutionary Strategy (MOEAS-PAES) and SPEA2. Thus, in order to improve the reliability and minimise the cost under uncertainties, this technique is implemented in designing of multi-microgrid systems considering wind turbine, solar photo-voltaic, and energy storage system in an active distribution electrical network [59]. The NSGA-II algorithm steps [29] are described as follows.

Step I: $S_T = Q_T \cup R_T$, perform non-dominating sorting to S_T and identify the different form of fronts $F_i(F_1, F_2, \ldots\ldots)$.

Step II: $Q_{T+1} = \phi$ and $i = 1$ until $|Q_{T+1}+|F_i < N$, $Q_{T+1} = Q_{T+1} \cup F_i$ and $i = i + 1$.

Step III: Perform crowding sort (F_i, α_c) and include most widely spread $(N- \mid Q_{T+1} \mid)$ remaining number of solution.

Step IV: R_{T+1} from Q_{T+1} using crowding distance (α_c) by tournament selection as follows:

(i) Rank of i $r_i <$ rank of jr_j (if to compare i, j with α_c). The non-dominating rank of i is always better than non-dominating rank of j. All the solution of fronts have the ranks 1, 2, ..., respectively.

(ii) If number 1 is not true or $r_i = r_j$, then $d_i = d_j$ which implies that the crowding distance is higher hence, it is required to improve the crowding population and widely spread population distance.

3.3.3 | Pseudo-random number generation

It is a procedure for generation of random variables in any kind of distribution system. It considers that an incidence is expressed as the outcome of two events which are mutually exclusive. The function shows that it works on a deterministic method which produces pseudo-numbers randomly and iterative as given in (12) [60].

$$y(n+1) = (i.x(n) + j) \bmod [n_k + 1], \tag{12}$$

where n_k is referred to as a number of cells in a WF, mod represents the remainder of the Euclidean division, n is the total number of WTs $< n_k$, and i, j are the positive integers. The ele-

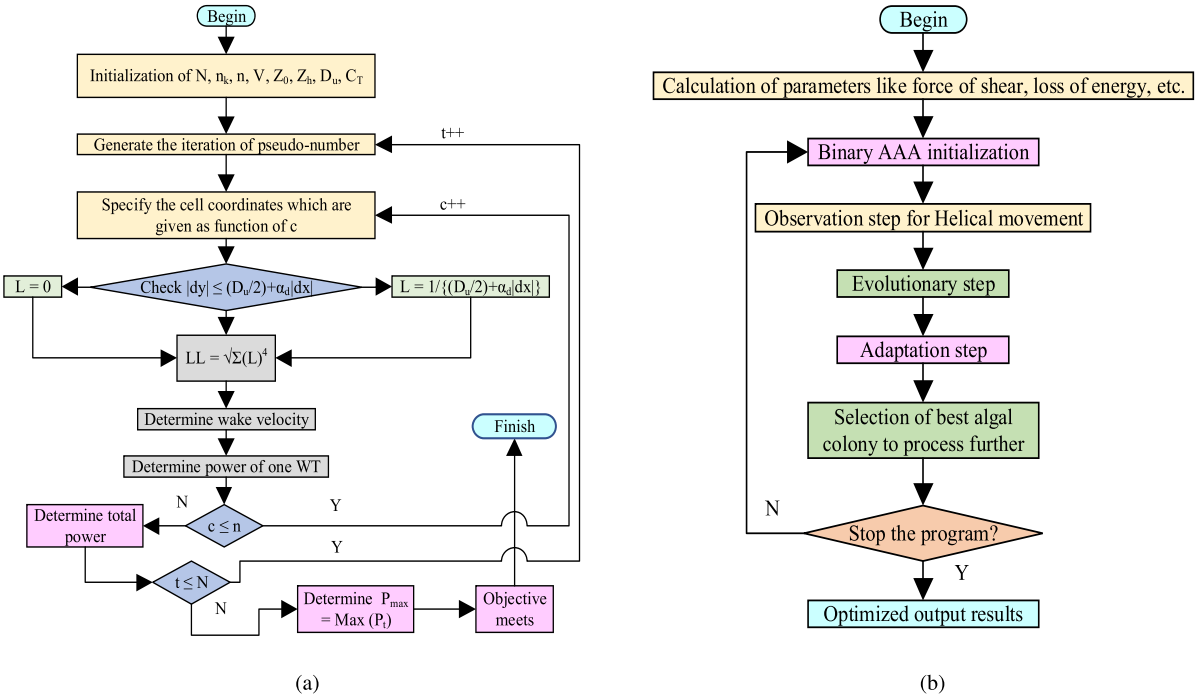

FIGURE 6 Algorithm for (a) PRN generation and (b) Binary Artificial Algae Algorithm

TABLE 5 Comparative analysis between PRN and GA (Moseti) [61]

Method	Cost/Total Power	Total Power (kW)	No. of WTs
GA (Moseti)	0.0016197	12,352	26
PRN generation	0.0015154	13,201	26

ments of this sequence are the remainders of the division on the divisor $(n_k + 1)$ and it is to be noted that $y(1) < (n_k + 1)$. As shown in flowchart Figure 6(a), this method is simple to program with less computational time which makes it suitable for engineering issues, especially in WF layout optimisation. Table 5 shows that an improvement of 2–6.5% in power production is observed for PRN generation method in comparison to GA [60, 61].

In PRN generation method, the following parameters are initialised first; N the number of iterations, n_k the number of cells in a square WF layout, n the number of WTs, V_d the velocity under wake effect, V the speed of the wind, D_u the rotor diameter, and C_T the thrust coefficient. Then the cell coordinates as a function of the rotor diameter and wake velocity (V_d) (13) are determined as described in the flow chart of Figure 6(a). The total power which is the sum of all WTs' power is determined as shown in (14) and (15) which is then utilised in finding the optimised value of the objective function (O.F.) as given in (16).

$$V_d = V\left[1 - \frac{D_u^{\,2}}{4}(1 - (\sqrt{1 - C_T}))LL\right], \tag{13}$$

$$\begin{cases} P_t = \sum \text{Power of single WT}(P_c) \\ P_{\max} = P_{t\max} \end{cases} \tag{14}$$

$$P_c = f(V_d), \tag{15}$$

$$O.F. = \text{Min}\frac{n\left(\frac{2}{3} + \frac{1}{3}e^{(-0.00175n^2)}\right)}{P_{\max}}. \tag{16}$$

3.3.4 | Binary artificial algae algorithm

The WT optimal placement for a 2 × 2 km area is designed. The surface of the area has been calculated by dividing the area into a 10 × 10 and a 20 × 20 grids. The use of binary coding algorithms, namely the BAAA, has been successfully applied to solve continuous optimisation problems [62]. This method is a combination of an evolutionary process, helical motion, and adaptation [63]. (17) is providing the algal population colony and result in a search space.

$$\text{Algal Colony Population} = \begin{bmatrix} a_1^{\,1} & \cdots & a_1^{\,d} \\ \vdots & \ddots & \\ a_n^{\,1} & \cdots & a_n^{\,d} \end{bmatrix}. \tag{17}$$

The proper result in a search space is given by $a_l = [a_l^{\,1}, a_l^{\,2}, \ldots\ldots, a_l^{\,d}]$ where, $l = 1, 2, \ldots\ldots, n$, $a_l^{\,k}$ is referred to as an algal cell in kth size or dimension of lth algal colony, D^d is the algal colony size, and n is the algal colony population. The problem dimension is equal to the algal cells present in any colony. The authors [64] have taken 10 new binary algorithms by using the same number of transfer functions of the AAA that is successfully implemented to solve the WT layout optimisation problem. The proposed method has achieved a 61% increase in total power in comparison to [20] and a 22.9% increase in comparison to [21] with a 9.8% increase in fitness value. The

TABLE 6 Comparative analysis between BAAA and other optimisation methods

Method	Cost/Total Power	Total Power (kW)	No. of WTs	Grid Size
GA (Grady) [20]	0.0015436	14,310	30	10 × 10
Parada [21]	0.0014940	14,785	30	10 × 10
Parada [21]	0.0014390	19,052	30	20 × 20
BAAA [24]	**0.0015414**	**14,667**	**31**	**10 × 10**
BAAA [24]	**0.0014054**	**23,422**	**49**	**20 × 20**
GA (Moseti) [61]	0.0016197	12,352	26	10 × 10
MILP [65]	0.0015436	14,310	30	10 × 10
BPSO-TVAC [66]	0.0015436	14,310	30	10 × 10
Lazy Greedy [67]	0.0015436	14,310	30	10 × 10

method is demonstrated with the help of a flow chart as given in Figure 6(b). Table 6 shows that the electrical power increases by 61% and 22.90%, respectively when BAAA is compared to Grady [20] and Parada [21].

3.3.5 | Non-linear mathematical model

The two objective functions are the maximum power output and minimum overall total cost which are considered and optimised as given in (18)–(23). The multi-objective optimisation problem is solved considering the rotor hub height and rotor diameter as the decision variables [56].

$$P_{l,k} = \frac{1}{2}\eta\rho A\left[u_0\left(1-\sqrt{\sum_{l=1}^{N}\sum_{k=1}^{N}\sum_{a=1}^{N}\sum_{b=1}^{N}V_{d_{lkab}}{}^2}\right)\right]^3, \tag{18}$$

$$\text{Max}\sum_{l=1}^{N}\sum_{k=1}^{N}\frac{1}{2}\eta\rho A x_{lk},$$
$$\left[u_0\left(1-\sqrt{\sum_{l=1}^{N}\sum_{k=1}^{N}\sum_{a=1}^{N}\sum_{b=1}^{N}x_{ab}.V_{d_{lkab}}{}^2}\right)\right]^3, \tag{19}$$

$$\text{Equation(16)} \tag{20}$$

$$\text{Min}\frac{\text{Equation(16)}}{\text{Denominator}} \tag{21}$$

where

$$\text{Denominator} = \sum_{l=1}^{N}\sum_{k=1}^{N}\frac{1}{2}\eta\rho A x_{lk},$$
$$\left[u_0\left(1-\sqrt{\sum_{l=1}^{N}\sum_{k=1}^{N}\sum_{a=1}^{N}\sum_{b=1}^{N}x_{ab}.V_{d_{lkab}}{}^2}\right)\right]^3,$$

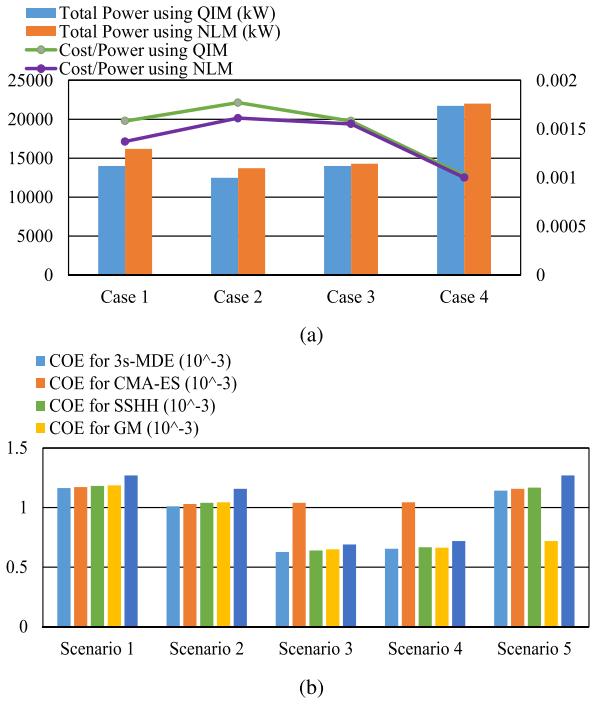

FIGURE 7 Comparative analysis of (a) QIM and NLM (b) GECCO-2015 competitors

$$\sum_{l=1}^{N}\sum_{k=1}^{N}x_{lk} \le T_N \tag{22}$$

$$x_{lk} \in (0,1);\ \forall\, l,k \tag{23}$$

where, $V_{d_{lkab}}$ is the velocity deficit in the wind speed due to WT at (a,b), η is the efficiency of WT, ρ is the air density, A is the cross-sectional area. The wind velocity is replaced by the velocity deficit in (19). The goal is to maximise the power and minimise the cost T_C by using (20) and (21) by locating WTs T_N (= n) at (l, k) positions. In [56], a method is suggested to eradicate the difficulty in non-linear power function. The binary decision variables of WT locations and implementation of the proposed method for 10, 20, 30, 40, 50 WTs. It eliminates the binary variables of WT (uni-modularity) but utilised the non-linear objective functions.

Figure 7(a) describes the dominance of NLM method in comparison to the quadratic integer model (QIM) method. The primary y-axis shows the total power in kW and secondary y-axis signifies the cost per generated power. Here, four cases are taken as follows.

Case 1: Wind speed is taken as 12 m/s with one north-south direction.

Case 2: Wind speed is taken as 12 m/s with 08 wind directions. These directions have an equal probability of occurrence.

Case 3: Wind speed is taken as 12 m/s with 36 wind directions. These directions have an equal probability of occurrence.

Case 4: Wind speed is taken as 8 m/s, 12 m/s, and 17 m/s with 36 wind directions. These directions have an unequal probability of occurrence.

3.3.6 | Genetic and evolutionary computation conference

The task of this conference [22] is to optimise the layouts of five generated WFs based on a simplified overall cost. The five WFs are based on the five scenarios which can be obtained from WindFLO repository. By scaling down the optimisation problem as a geometric optimisation problem. The four algorithms are chosen and described in this subsection which was developed by the conference competitors. The task given in this competition is to minimise the cost of energy F as described in (24). Figure 7(b) describes a comparative analysis of genetic and evolutionary computation conference (GECCO) competitors in the given five scenarios.

$$F = \left(\frac{(C_T N + C_S \left\lfloor \frac{N}{M} \right\rfloor) + C_{OM} N}{\frac{1-(1-R)^{-Y}}{R}} \right) \frac{1}{8760W} + \frac{0.1}{N}, \quad (24)$$

where C_T describes cost of WT, N is the number of WTs in WF layout, C_S gives substation cost which is the function of floor value of N/M, M is the number of WTs at each substation, C_{OM} refers OM costs, R is the rate of interest, Y is the WF life, W gives the total output energy of WF layout.

(1) *3 stages memetic differential evolution*: The termination criterion of the local search in MDE determines the allocation of limited computational resources between global and local search, and has a tremendous impact on the optimisation performance [68]. An improved CMA-ES has also been suggested for large-scale optimisation solutions. 3 stages memetic differential evolution (3s-MDE) estimates the cost function and then MDE is utilised to optimise the WF layout model as described in the flow chart of Figure 8(a).
(2) *Co-variance matrix adaptation-evolution strategy*: Co-variance Matrix adaptation-evolution strategy (CMA-ES) uses the co-variance matrix to optimise the layout model which use the horizontal scale, vertical scale, relocate from the origin, relocate from a location, and rotation as five variables. The candidate solution x_{ik} of i_{th} sample is given in (25).

$$x_{i\to k}^{k\to t} \sim \nu(m^t, \sigma^t C^t) = m^t + \sigma^t \nu(0, C^t). \quad (25)$$

For tth iteration, a mean m^t of the distribution is utilised to generate λ candidate solutions $x_k \in R^n$ by adding a random Gaussian mutation defined by a co-variance matrix $C^t \in R^{n*n}$ where σ^t is a mutation step size and λ solutions are then calculated on an objective function. It also optimises the number of WTs and their locations which uses five variables to parametric search space of WF layouts. The variables are used to:

(i) Complete a rectangular layout grid of WTs,
(ii) Relocate it back to the beginning,
(iii) Revolve it,
(iv) Move it to any other location.

(3) *Sequence-based selection hyper-heuristic*: Sequence-based selection hyper-heuristic (SSHH) discretises the WF layout into three variables namely the distance between the adjacent WTs and the shift factor. Additionally, this selection method uses the Markov model to produce a series of low-level heuristics to form a final WT layout. It mainly represents a learning series of an acceptance method and heuristic selection method to resolve the WT layout optimisation problem.
(4) *Goldman method*: To evaluate the WT locations and substation cost, Goldman method (GM) uses a pair of lattice vectors with their optimisation.

3.3.7 | Multi-objective PSO

In this method, the particles are having a potential solution and this is considered in the WF layout optimisation problem. The hybrid multi-objective meta-heuristic algorithm, which is based on non-dominated sorting multi-objective PSO (MOPSO), is proposed to find the optimal WT layout [69]. WT locations are searched in the continuous space as described in Figure 8(b) [70]. The PSO algorithm flow chart deals with the finding of the power output of the wind farm (POWF) which is a function of wind direction θ_i, wind speed V_i, and the turbine location x_m. An equivalent power of a wind farm has been obtained using POWF, number of considered wind direction N_d, number of considered wind speed N_s, and number of turbines N_p.

The Pth swarm particle represents a Z_p vector and the individual particle is calculated by using the objecting and adopted with the help of position and velocity update as described in (26)

$$V_p^{i+1} = \omega V_p^i + \psi_1 (P_p^i - Z_p^i) U[0,\ 1] + \psi_2 (P_g^i - Z_p^i) \quad U[0,\ 1], \quad (26)$$

where ψ_1 and ψ_2 determine the global and personal best particles, $U[0, 1]$ is the actual value which is selected in every uniform wind velocity from the interim of [0, 1]. The position swarm particle p in the upcoming iteration is $Z_p^{i+1} = Z_p^i + U_p^{i+1}$. Using the above, the two objective functions are solved.

4 | RELIABILITY ASSESSMENT OF WIND INTEGRATED POWER SYSTEM (WIPS)

This paper has discussed the various wake models with their effects on WF planning in Section 2 and different optimisation techniques to obtain the optimal WF layout in Section 3. Now, it is required to ensure the proper working of the main power system when it is integrated with a WF considering the optimised layout. The integration first leads to consider the

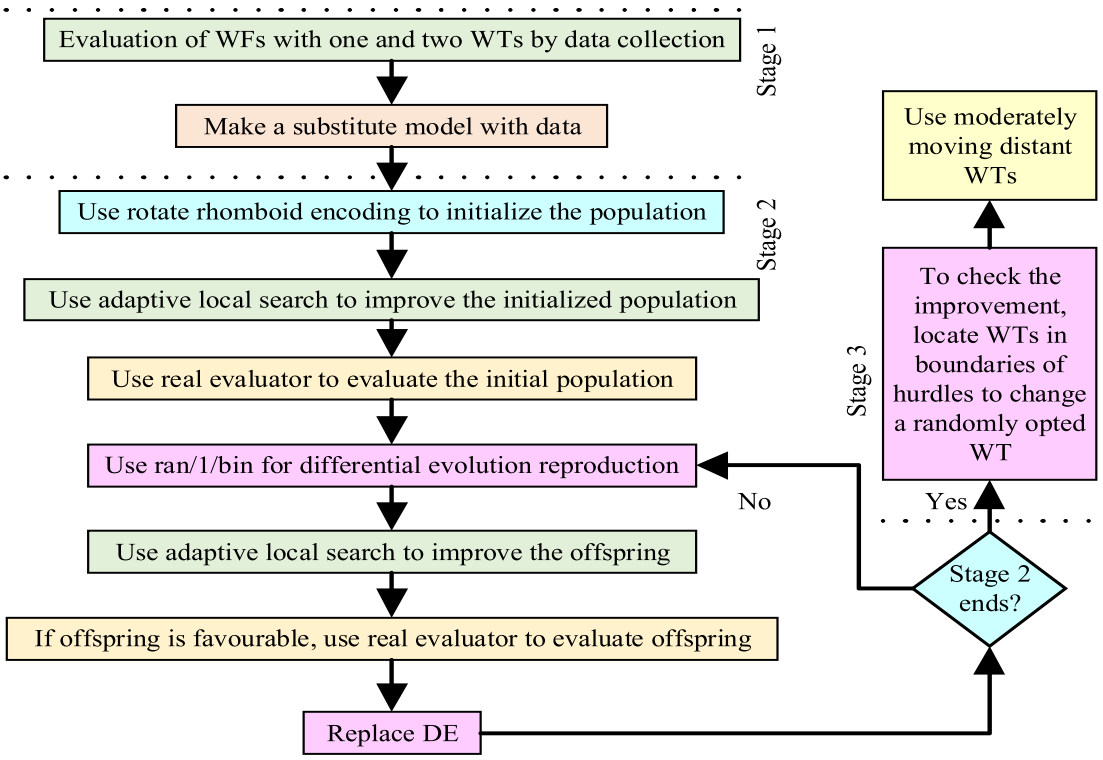

(a)

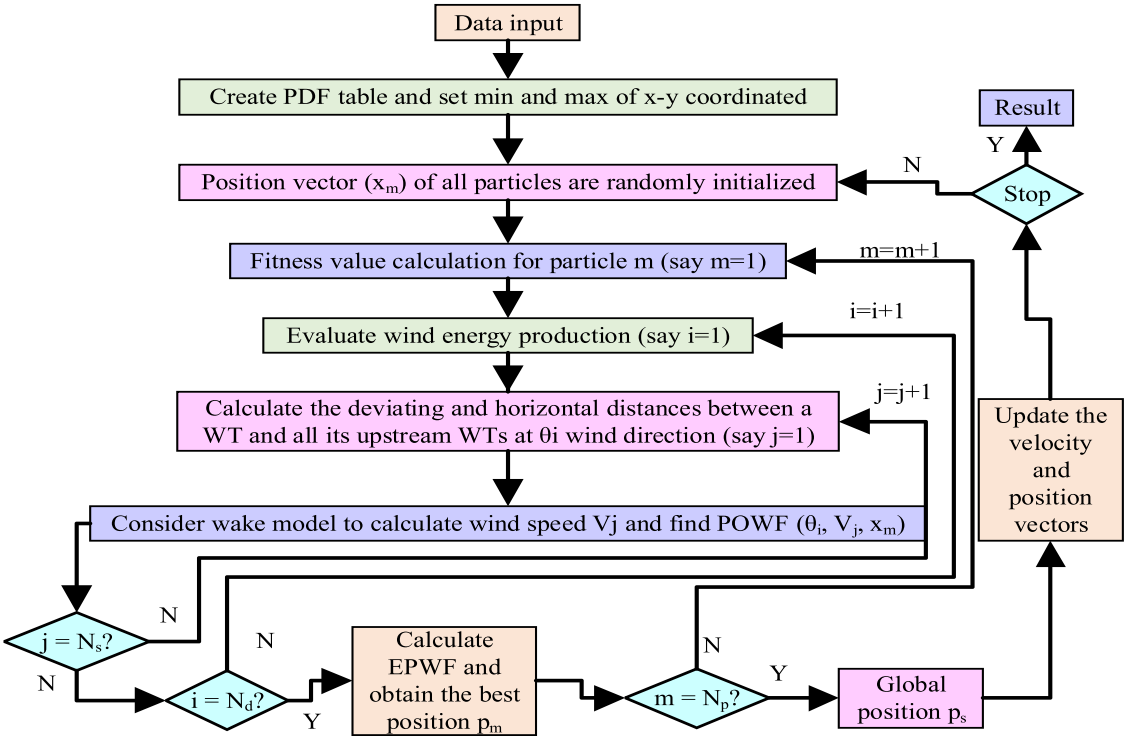

(b)

FIGURE 8 Algorithm for (a) 3 stages memetic DE algorithm (b) Multi-objective PSO algorithm

optimal location of WF in the conventional power system. After getting the optimal WF location, it becomes a tedious scenario where parameters related to generation and transmission must meet their constraints for the WIPS. However, due to the uncertainties involved in WF, an issue related to generation reliability occurs in a WIPS. So, the discussion of this paper is solely concentrated on reliability evaluation and improvement of OWF and WIPS and this section provides an overview of reliability studies [71].

4.1 | Off-shore WF reliability assessment and cost analysis

According to [72], reliability is the probability that a WT has an operational path up to the Point of Connection Coupling. The Generation Ratio (GR) which defines the performance of the electrical system is shown in (27). The inclusion of optimally designed WF into the conventional power system leads to perform the reliability assessment of a generating system comprising a WF. Moreover, the failure of a WT earns interest in the study of system adequacy analysis. Following the reliability evaluation, the cost analysis is necessary to study because of the higher cost involved in OWF development. Thus, both scenarios are discussed in this subsection with supporting mathematical models. Also, an accurate reliability assessment method is proposed for the electrical power system consisting of conventional generators, WT, Solar PV, and the ESS [73].

$$GR = \frac{P_d}{P_g}, \tag{27}$$

where P_d is referred to as the power delivered which is evaluated by obtaining the reliability of each minimal path between WT and the junction of common coupling onshore and P_g is referred to as power generated which is the total effective power produced by the WTs.

4.1.1 | Economic and reliability models

In [74], optimised WF architecture is developed which is then compared to the actual farm in France, namely 'Banc de Guerande', by considering the cost and reliability optimisations which are taken into account to study the OWF performance and design analysis. The main task is to incorporate the WF topology and reliability data of components to analyse the WF performance with cost minimisation. The steps to obtain the reliability indices by finding the minimum paths between the sink and sources are as follows:

Step I: Connection to the network
Step II: Produce a reliability block diagram
Step III: Obtaining all minimal points between sources and sinks
Step IV: Include reliability data for the calculation of reliability indicators

TABLE 7 Comparative analysis of GA optimisation results between cases A, B, C and reference [74]

Quantity	Reference	Case A	Case B	Case C
Investment cost (M€)	261	243	320	307
LPC (€/kWh)	0.00769	0.00781	0.00927	0.00885
EENS (MWh/year)	0.19520	0.33787	0.16825	0.16589
Total Cost (M€)	938	1415	904	883

Table 7 represents the reliability and economic assessment of a 3-bus OWF structure. The reliability data is adapted from [75]. In this tabular interpretation, Case A is for investment cost optimisation with the variation in number and position of Offshore Electrical System (OSS), Case B is for optimisation of starting cost plus Expected Energy Not Supplied (EENS) cost without considering variation in number and position of OSS, and Case C is for optimisation of starting cost plus EENS cost considering variation in number and position of OSS.

Further, some assumptions are taken to calculate the reliability which are as follows:

(i) The bus bar, generator, cable, transformer, switch, breaker, etc., are considered either ON or out of service (maintenance or repair)
(ii) It is also assumed that all components are independent and work on their maximum power rating which implies no overload condition
(iii) The repair and failure rates are considered to be constant during the OWF lifetime

The system status function for reliability calculation is given in (28) and the subsystem availability with EENS, Annual Outage Hour (AOH), and Equivalent Availability Factor (EAF) is defined in (29)–(32).

As it is mentioned in [2] that Reliability Based Design optimisation (RBDO) is implemented to reduce the OM cost which is 25–28% of total cost, then it becomes necessary to model the total investment cost which includes the variable parts, that is, cables and OSS as given by (33) and Levelised Production Cost (LPC) is determined by (34).

$$\Phi_{ss,j}(x) = 1 - \left(1 - \prod_{i \in MP_1} X_i\right)\left(\prod_{i \in MP_2} X_i\right) \ldots \ldots \left(\prod_{i \in MP_k} X_i\right), \tag{28}$$

where X refers to the status of the component (1 for working and 0 for not working), n is the number of components, j is subsystem number, and k is the number of MPs.

Subsystem Availability:

$$A_{ss,j} = \frac{\mu_i}{\mu_i + \lambda_i} + \frac{\lambda_i}{\mu_i + \lambda_i} e^{-(\mu_i + \lambda_i)t}, \tag{29}$$

where, μ_i and λ_i are termed as failure and repair rates, respectively, the inverse of μ_i and λ_i are defined as the average time to failure and average time to repair, respectively.

$$EENS = \sum_{j=1}^{N_s}(1 - A_{ss,j})P_{WT,j} \times 8760, \tag{30}$$

where $P_{WT,j}$ is the power of jth WT.

$$AOH = \frac{EENS}{\sum_j^{N_s} P_{WT,j}}, \tag{31}$$

$$EAF = 1 - \frac{AOH}{8760}, \tag{32}$$

$$C_{\text{invest}} = \frac{r.(1+r)^T.T}{(1+r)^T - 1}.\frac{1}{1-PR}.C_0, \tag{33}$$

$$LRC = \frac{C_{\text{invest}}}{E_d(C_t)}. \tag{34}$$

Mean Energy Produced is then calculated in (35):

$$E_d(C_t) = P_{\text{mean,out}}(C_t).N_t.T - EENS.T, \tag{35}$$

where C_0 is the initial investment, r is the percentage rate of interest, PR is the percentage annual profit, T is the lifetime of WF (generally taken 20 years), $P_{\text{mean, out}}$ mean power produced, N_t is the number of WTs, C_t refers as the connection topology.

The OWF electrical design is a complex problem, hence some previous works consider the following simplifications during the layout optimisation problem.

(i) Voltages are fixed in MV sides
(ii) WTs produce constant power
(iii) WTs are connected radially
(iv) Number of WTs is fixed

Further, paper [32] has developed an optimisation model of a standalone PV-wind system using NSGA-II and considered the feasibility of cost and reliability of the overall system. It is also mentioned that the constraints and objectives in an optimisation problem are classified into cost, reliability, and environmental indices. Cost indices are used to analyse the cost viability of the system, the environmental index is applied to mention the impact on the system, and the reliability indices are utilised to describe the capability of a system to react to the power demand in an efficient and continuous mode.

4.1.2 | Considering wake effect only

Authors have opted WFs from three sites in America and incorporated these into the IEEE RTS and RBTS with a yearly peak load of 185 MW and 2850 MW, and rated capacity of 240 MW and 3405 MW, respectively [70]. The wake creates reduction in the annual energy production of a WF. Thus, the optimal placement of the WTs considering wake effect is a major concern to obtain the maximum energy at minimal cost [76]. Authors of [77] have given data and load curve for basic reliability. The reliability function includes wake effect and WTGs' failures and determines the reliability indices as illustrated in (36)–(39).

$$LOLP = \frac{1}{n_r}\sum_{j=1}^{n_r} i(P_{\text{load}_j} - P_{\text{wind}_j} - P_{\text{gen}_j}), \tag{36}$$

$$LOLE = \frac{t}{n_r}\sum_{j=1}^{n_r} i(P_{\text{load}_j} - P_{\text{wind}_j} - P_{\text{gen}_j}), \tag{37}$$

$$EENS = \frac{t}{n_r}(P_{\text{load}_j} - P_{\text{wind}_j} - P_{\text{gen}_j})\sum_{j=1}^{n_r} i(P_{\text{load}_j} - P_{\text{wind}_j} - P_{\text{gen}_j}), \tag{38}$$

where P_{load_j}, P_{wind_j}, P_{gen_j} are load of the system, WF power output, main generator power output, respectively in time t. i is an indicator, which is defined in (39) as

$$i(P_{\text{load}_j} - P_{\text{wind}_j} - P_{\text{gen}_j}) \tag{39}$$

$$= \begin{cases} 1, & (P_{\text{load}_j} - P_{\text{wind}_j} - P_{\text{gen}_j}) > 0 \\ 0, & \text{Otherwise.} \end{cases} \tag{39}$$

4.1.3 | Wind Turbine failure under wake effect

The output of a WTG is affected by wake due to upstream WT and the situation becomes observable when WT in the WF fails. It leads to change in power output due to different wind speed distribution towards the downstream WTs. To analyse this scenario, an MCS method is proposed for adequacy analysis [10] as shown in Figure 9. The reliability indices are calculated to depict adequacy of generating systems to provide a given load as given in (40)–(43). A comparison of reliability indices for WF integrated IEEE-RTS is shown in Table 8.

$$LOLE = \frac{1}{n}\sum_{j=1}^{n} LOLE(X_j), \tag{40}$$

$$LOLP = \frac{LOLE}{n}, \tag{41}$$

$$EENS = \frac{1}{n}\sum_{j=1}^{n} EENS(X_j), \tag{42}$$

$$LOLE = \sum_{j=1}^{n} A_j P_j. \tag{43}$$

where X_j is the state value of jth period and n is the total period. $LOLE(X_j)$ and $EENS(X_j)$ are the Loss of Load Expectation

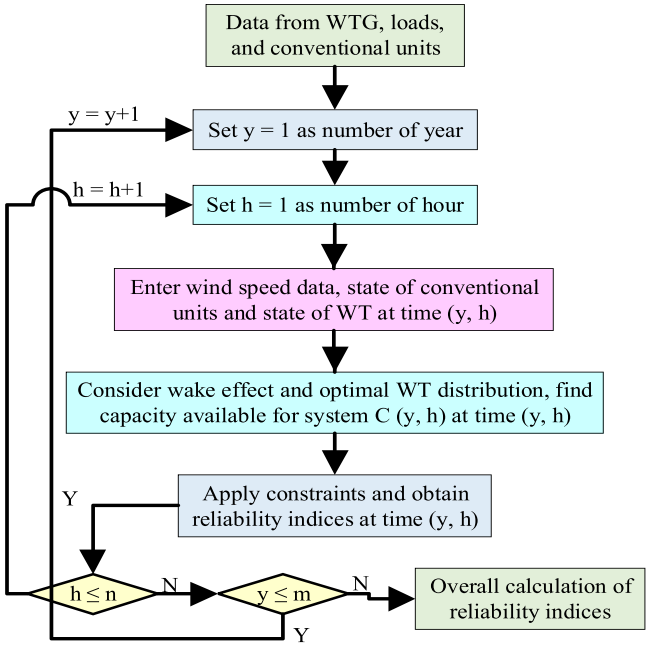

FIGURE 9 MCS algorithm for adequacy analysis

TABLE 8 Comparative analysis of reliability indices obtained during cases A, B, C, D and E [10]

Cases	LOLE (hours/yr)	$LOLP \times 10^{-3}$	$EENS \times 10^3$ (MWh/yr)	$EEP \times 10^3$ (MW/yr)
Case A	6.83	782	0.6330	148.910
Case B	7.40	847	0.6980	56.753
Case C	7.55	864	0.7010	53.675
Case D	6.89	789	0.6636	113.280
Case E	6.92	792	0.6635	110.070
Layout	Total Power output (MW/year)			
Original	54.558×10^3			
Optimal	108.890×10^3			

(LOLE) and EENS values at jth period. A_j is the WF capacity produced in jth state, P_j is referred as the probability of the jth capacity state, and m is the total number of capacity states.

4.1.4 | Cost analysis

Economic and reliability analysis for WT system has already been considered in the literature [78]. It is mentioned in the literature that for the same capacity, the cost of Off-shore WF is 30–60% greater than the onshore WF. The cost percentage involves in WF includes the cost of the turbine with its transportation and installation 49%, the cost of foundation with WF to grid connection 37%, the internal connections between WTs 5%, project management with environmental analysis 3% and miscellaneous 1%. So, it is required to take economic study in consideration which depends on various factors including AC or DC system, length of transmission, transmission voltage, rated power, type of WT, WF layout, and speed of the wind. Figure 10 shows a flow of WT economics which depicts the saving of € 38.0574 per MWh in annual maintenance cost and profit of € 18.7452 per MWh in increased annual electricity production. [79].

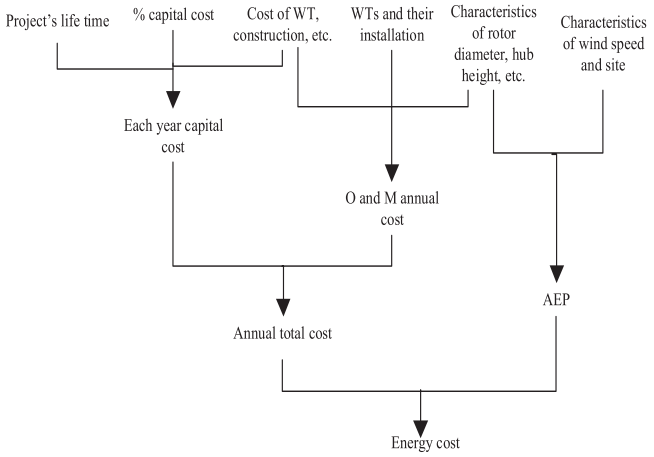

FIGURE 10 An overview on WT cost

Some researches have done a cost modelling and analysis which also relates to the reliability of the system. Firstly, a cost model is developed as described in (44) and (45) and then cost analysis is performed which are given in (46) and (47). On the other hand, an MCS model flow chart is given in Figure 11 which considers probability distribution of air-density, wind speed, Weibull shape parameters, rough of the sea surface, and WT power to evaluate the reliability index AEP. In this MCS-based algorithm, P_t refers point, and Y_r signifies year. Further, it is delineate that with the inclusion of WF, the minimum and maximum energy cost (€ /MWh) decreases from 0.045 to 0.03825 and 0.117 to 0.05175, respectively, for the same total generation (MW) [80].

$$\text{Cost of transformer} = a_P + b_P P_{\text{rated}}{}^{\alpha}, \tag{44}$$

$$\text{Cost of Cable} = \varkappa_P + y_P \exp\left[\frac{\varkappa_P P_{\text{rated}}}{10^8}\right]. \tag{45}$$

The cost modelling is given for the transformer and cable, where offset constant $a_P = 0.205 \times 10^6$, slope constant $b_P = 364.6$, $\alpha = 0.4473$ and P_{rated} is the rated output power. $\varkappa_P$, y_P and $\varkappa_P$ are constants.

$$\text{Cost of wind energy generated} = \frac{c_I}{(AEP)}\left[\left(\frac{i(1+i)^m}{(1+i)^m - 1}\right) + m\right], \tag{46}$$

where c_I is initial cost of WT, i is the % interest rate, and n refers to OM cost.

$$c_I = 1.15(c_t + c_F + c_{\text{Ins}} + c_G). \tag{47}$$

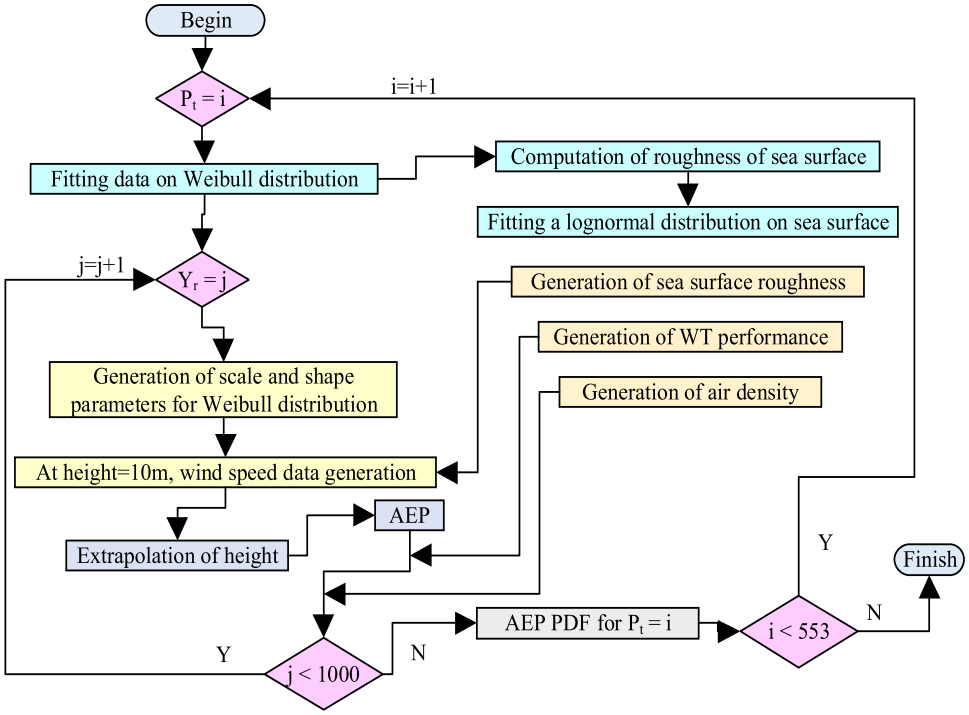

FIGURE 11 MCS algorithm based on probability models

The initial cost c_I is the total sum of WT cost c_t, installation cost c_{Ins} and grid connection cost c_G. The task to minimise the Net Present Value (NPV) is done [81] and summarise the cost analysis involved during WT performance. The objective function is defined as

$$^{\text{minimum}}NPV_{\text{Total}} = NPV_{\text{Comp}} + NPV_{\text{LoadLoss}} + \text{Retribution Value}, \quad (48)$$

$$NPV_{\text{Comp}} = V_{\text{Cap}} + V_{\text{Main}} + V_{\text{Rep}}, \quad (49)$$

$$NPV_{\text{LoadLoss}} = LOEE \times V_{\text{LoadLoss}} \times (AVP), \quad (50a)$$

$$V_{Cap} = V_{WT} \times n_{WT}, \quad (50b)$$

$$V_{\text{Main}} = AVP \times (V_{WT} \times n_{WT}), \quad (50c)$$

$$V_{\text{Rep}} = C_P \times (V_{WT} \times n_{WT}), \quad (50d)$$

where NPV_{Total} is the total net present value of a WT, NPV_{Comp} refers to net present value of WT system components as given in (49), NPV_{LoadLoss} is the net present value of loss of load. The NPV of components includes capital, maintenance, and repair values and are denoted by V_{Cap}, V_{Main}, and V_{Rep}, respectively. Further, the values are described in (50a)–(50d) where AVP and K are the annual value payment and constant payment, respectively. V_{LoadLoss} is the disconnection value per kWh of load demanded. V_{WT} and n_{WT} are the value of each WT per year and number of WT, respectively. Finally, it is clear from (48) that to meet the reliability constraints, the retribution value must be equal to 0.

In this article, the main indices LOLE (hour/year) and Loss of Energy Expectation (LOEE) (kWh/year) are discussed as two reliability constraints [82, 83] and these are defined as given in (51a) and (51b).

$$LOLE = \sum_{T=1}^{n} LOLE(T), \quad (51a)$$

$$LOEE = EENS = \sum_{T=1}^{n} LOEE(T). \quad (51b)$$

5 | RELIABILITY IMPROVEMENT METHODS

This paper illustrate the four reliability improvement techniques briefly. The advantages and disadvantages of all techniques are described in Table 9.

5.1 | Generation rescheduling Algorithm

Generation rescheduling Algorithm (GRA) is applied in [84], which provides adjustable output generation to remove the fluctuations of power flows through the transmission line and simultaneously, the probability of overloading is relieved. This algorithm is used to schedule the conventional generation in order to increase the transmission system reliability with

TABLE 9 Advantages and disadvantages of reliability improvement methods

S. No.	Method	Advantage	Disadvantage
1	GRA	(i) Power flow variations are taken out from the transmission line. (ii) It minimises the probability of overburdening. (iii) Increases the transmission system reliability	Gives a flexible output power generation by ignoring the congestion in power, and stabilises the wind energy resources with power system loads.
2	Demand Side Management (DSM)	(i) It evaluates the load side reliability. (ii) Reliability increases for the combined stage of hybrid energy and DSM.	(i) Users have a restricted resource to use the DSM. (ii) DSM is a better fit for greater energy consumers or those with complex energy demands.
3	EV	(i) The reliability of an electrical distribution system enhances using V-G and V-H concepts. (ii) This method of reliability improvement is efficient in long term operation.	(i) The maintenance cost is higher for EVs.
4	ESS	(i) It includes reliability enhancement with analysing the power system service recovery. (ii) It utilises the parking lot as a substitute for a disturbed zone.	(i) Energy loss in charging–discharging makes it inefficient. (ii) It is complex and not cheap and requires infrastructure and space.

renewable energy penetration. Although GRA is mainly useful in preventing the congestion in power and the balance in Distributed Energy Resources and power system loads, one of the previous methods like Participation Factor Control (PFC) is unable to consider the locations of the generators. Hence, the GRA to increase the reliability with load and wind power uncertainty is developed. Overall, the GRA is applicable in determining the optimal generator rescheduling solution. It is useful for mitigating the overloading scenarios and minimising the weighted sum of branch power flow variances. The method is explained briefly in Figure 12(a).

5.2 | Demand side management

Demand side management (DSM) is a long-term reduction in customer load as compared to demand response which adjusts the peak load only. To assess the load side reliability, the DSM method is given [85] which is applied to the Electrical Power Distribution System (EPDSs) to achieve the efficient reliability of the power system. On the other side of the analysis, DSM is also considered for control of microgrid considering Battery Energy Storage System (BESS), protection, and power quality issues [86]. Thus, MCS and a local load system method are developed for reliability evaluation and assessment, respectively, which incorporates DSM and wind as described in Figure 12(b). This MCS-based algorithm for DSM calculates the failure CDF F(t), and repair CDF R(t) using simulated hour t in the year, the total number of simulated hours T in the year, and randomly generated number U between 0-1. The DSM method modelling is applied to get the improved load reliability index called Energy Not Supplied (ENS) [87]. Loss of Load Probability (LOLP) and normalised generation has been improved by using DSM. The reliability improvement is also seen in [88] where IEEE-RTS is taken with and without the integration of wind energy to see the impact on reliability indices including LOLE (hour per day), Energy Demand Not Supplied (MW), Expected Energy Not Recovered (MWh) and EENS (MWh/year).

5.3 | Electric Vehicles

The impact of Full EVs and Plug-in EVs have been considered for EPDS reliability improvement and greenhouse gas mitigation [89]. Authors of [90] have suggested integrating EV in different modes of operation such as centralised and dispersed EV charging in which residential demands are fulfilled by V-H or/and V-G during the is-landing condition. In sequence to this, as a part of planning, the reconfiguration of the electrical network for the improvement of system reliability is presented and the implementation of V-G programs of EVs is effectively considered in [91] and [92], respectively. These studies are for reliability and adequacy analysis of EPDSs.

A stochastic traffic flow model is elaborated under two scenarios. First, the influence of time interval of reliability information on the traffic flow system. Second, the impact on the stability of the traffic system, which provides the significance of information reliability on the stability of traffic stream by using analytical methods [93]. Therefore, to solve the mentioned problems on optimal velocity and the dynamics of information reliability, some techniques related to EVs are developed. The two car-following models are given and explained in (52)–(54).

$$\frac{dv_k(t)}{dt} = \gamma(V(\Delta S(t)) - v_k(t)), \tag{52}$$

$$V(\Delta s_k) = \frac{v_{\max}}{2}(\tanh(\Delta s_k - s_c) + \tanh(s_c)), \tag{53}$$

$$\frac{dv_k}{(t)}dt = \gamma\left(V\left(\sum_{L=1}^{P}\alpha_L\eta_L\Delta s_{k+L-1}(t)\right)\right), \tag{54}$$

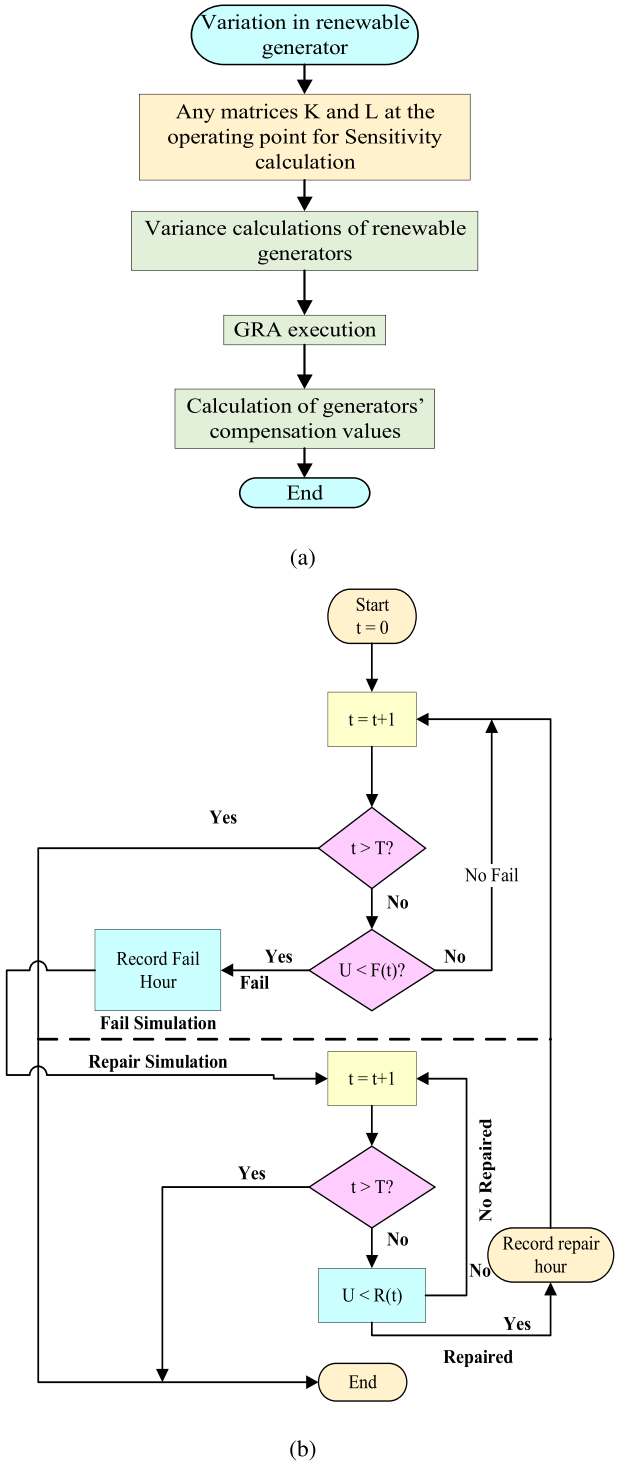

FIGURE 12 (a) Algorithm for GRA execution. (b) Monte-Carlo simulation implementation in DSM

where γ is constant which is termed as driver's sensitivity. s_k is the distance of kth vehicle. v_k is the kth vehicle velocity. Δs_k is the head-to-head distance between k vehicles and its immediate next vehicle ahead. $V(*)$ is the expected velocity which is dependent on Δs_k. s_c is the distance of safety. α_L is a variable which shows the information which is shared by Lth vehicle, if available. η_L is the coefficient of influence of the Pth preceding vehicle on other vehicles. P is the Pth vehicle which is coming before of present vehicle k, where, $L < P$; $L \in 1, 2, 3, \ldots, P$.

The charging load of EVs has challenges in electrical power system operation, electricity market, and planning due to the imbalanced spatial distribution of electric vehicles. The MCS method is suitable to determine the charging time span and charging power of EV which is completely dependent on the probabilistic distribution of Conventional Vehicle. The (55) and (56) show the charging start time and PDF of daily mileage, respectively.

$$f_x(y) = \begin{cases} \frac{1}{\sigma_x\sqrt{2\pi}}\left[\exp\left(-\frac{(y-\mu_x)^2}{2\sigma_x^2}\right)\right]; \ \mu_x - 12 < y \le 24 \\ \frac{1}{\sigma_x\sqrt{2\pi}}\left[\exp\left(-\frac{(y+24-\mu_x)^2}{2\sigma_x^2}\right)\right]; \ 0 < y \le \mu_x - 12 \end{cases} \tag{55}$$

$$f_{\tilde{x}}(y) = \frac{1}{y\sigma_{\tilde{x}}\sqrt{2\pi}}\left[\exp\left(-\frac{(\ln y - \mu_{\tilde{x}})^2}{2\sigma_{\tilde{x}}^2}\right)\right], \tag{56}$$

where P_E denotes electricity price, α_p and β_p are referred to standard deviation and the expected value of the electricity price, σ_x, σ_Z, and μ_Z are the respective shape-parameters.

The incorporation of V-H and V-G into the EPDSs for reliability where V-G is to support the grid during outages by providing the frequency regulation and spinning reserve [94]. The dependence of energy quantity available from EVs is on the duration of outages, charging requirement time, and spatial patterns. Electric V-H acts as an energy source to supply household demand and when the numerous nodes are incorporated in inter-regional V-G. If the loss of power along the line are involved, then the issue is being treated as an optimisation problem. In this optimisation problem, the only objective is to decrease the residual ENS at all nodes. The aim of non-linear optimisation [95] is to minimise the losses over the power network throughout EV charging. The power flow calculation uses the quadratic programming technique which serves as the most effective tool. An iterative backward-forward sweep method is applied in power flow calculation for better results. On the other study of optimisation, the interior point method is described to obtain the optimum values while in each try an optimal flow algorithm is run to get the maximum power imported at each node of the system [96]. In the EV charging, the reliability of the EPDS is improved together with the basic participation of EVs, that is, V-G in local for centralised charging of EV and V-H for distributed EV charging. The Sequential Monte-Carlo Simulation method for the assessment is provided with reliable results. The involvement of local V-G for centralised charging and local V-H for dispersed charging leads to the reliability improvement of EPDS. The EPDS has gained interests as EV industries with large power capacities and energy are growing frequently.

The interfacing between transportation infrastructure, and energy consumers, and generating units are the different forms of energy in an energy hub [97]. A renewable-based energy hub concept is considered for modelling the interactions between various Distributed Generation technologies. The related reliability indices System Average Interruption Duration Index

(SAIDI) and EENS during grid-connected and is-landed conditions are given and the implementation of the proposed framework is done. The calculation of reliability indices and the test system is calculated by taking various working energy hub strategies. Thus, the reliability improvement of energy demands is achieved by using co- or tri-generation converters in an energy hub. At last, the reliability is also improved by energy hubs which are dependent on the component's reliability, energy networks' level, and operation planning [92].

5.4 | Energy storage system

Power system reliability improvement analysis is performed considering the energy storage system (ESS). Authors in [98] have obtained reliability indices and performed several ESS-based network configurations to increase the EPDS reliability. A methodology was described for a probabilistic EPDS reliability evaluation using an MCS method in case of multi-ESS installed at WFs. The ESS includes the battery and hydro-pumped. A brief review based on ESS is done [99]. A probabilistic forecast methodology of an energy resource is developed to analyse the O and M of the wind energy system with the storage system [100]. Further, considering battery state of charge, reliability indices including SAIDI (hour per customer per year), ENS (MWh per year), and Contingency Occurrence Rate (contingent failure per year) have been obtained [101]. An MCS technique is given to analyse the power system impacts of wind energy on the reliability benefits from the ESS. The SAIDI and total reliability costs are minimised where the cost is dependent on the aggregate interruption cost of the customer. The aggregate interruption cost includes PL installation cost and incorporation cost of a PL. The PL acts as a unit that provides the back-up for the interrupted zone (reduces the interruption time) and acts as a unit that provides the storage in the back-up feeder (reduced the congestion frequency). The voltage deviation and energy costs are also taken into account during reliability cost determination. The overall objective function is the combination of operative objective and objective based on reliability. The stochastic model and MCS technique are proposed [102] which is useful in determining the PL effects to nearby services on reliability enhancement with the consideration of service restoration. The reliability-based objective functions Electric Vehicle Parking Lot Allocation Program allocation problem is described in (57) and (58), where the minimisation of two reliability indices E_{SAIDI} and E_{T_C} is accomplished for reliability improvement.

$$O.F.^{\text{rel}} : \left\{ \alpha_1 \left(\frac{E_{T_C} - T_{C_{OPT}}}{T_{C_{OPT}}} \right) + \alpha_2 \left(\frac{E_{SAIDI} - SAIDI_{OPT}}{SAIDI_{OPT}} \right). \right) \tag{57}$$

$T_{c_{OPT}}$ and $SAIDI_{OPT}$ are determined optimally by putting any of the weighting factors 'zero' [103].

$$E_{T_C} = E_{T_{IC}} + E_{T_{PlC}} + T_{IMC}, \tag{58}$$

where, E_{T_C}, $E_{T_{IC}}$, $E_{T_{PlC}}$, and T_{IMC} are the expected overall reliability cost, interruption cost, PLs incorporation cost in service restoration, and overall investment and maintenance costs of PL.

6 | CONCLUSION AND SCOPE FOR THE FUTURE WORK

This paper has drawn interest in the types of WTGs and wakes developed towards downstream rotors due to the front WT rotors. By virtue of the turbulence behind the upstream WT rotor, there is a disturbance in the inflow wind of downstream rotors which creates deficit velocity, and hence, the decrease in WT output power is observed. Thus, the solution to get the maximum power is considered by developing an optimal WF design. To achieve this, some optimisation techniques have been discussed to get the optimal design of WF at minimum cost per total power. Simultaneously, the system's reliability has also taken as a primary concern after observing the occurrence of improper calculations of reliability indicators due to the presence of uncertainties in WF. Thus, the reliability study and its improvement techniques have been discussed.

On the basis of this research review, the following suggestions are recommended for future study and industrial reliability needs.

i. Research can be extended to implement different or realistic wake models other than simple Jensen's model to obtain the WT locations for an optimal WF design.

ii. Considering probabilistic scenarios to find the WF optimal location in the main power system (RBTS and IEEE RTS) is also a topic to work upon.

iii. The implementation of EVs and BESS as the reliability improvement techniques in WIPS is also a challenging issue in terms of their optimal locations.

iv. Study on Reliability Availability Maintainability is one of the major topics to get the proper cost analysis on WF design.

ACKNOWLEDGMENTS

The authors wholeheartedly thank the Department of Electrical Engineering, Indian Institute of Technology (Banaras Hindu University), Varanasi for providing the laboratory-related facilities to accomplish the research work in time. The first author expresses his gratitude towards Govind Ballabh Pant Institute of Engineering and Technology, Pauri Garhwal, Uttarakhand, India for giving him the opportunity to pursue a PhD from IIT (BHU) Varanasi, Uttar Pradesh, India.

ORCID

Sachin Kumar https://orcid.org/0000-0003-1517-7450
R.K. Saket https://orcid.org/0000-0002-2773-9599
Dharmendra Kumar Dheer https://orcid.org/0000-0001-6231-8813
P. Sanjeevikumar https://orcid.org/0000-0003-3212-2750
Jens Bo Holm-Nielsen https://orcid.org/0000-0002-0797-9691
Frede Blaabjerg https://orcid.org/0000-0001-8311-7412

REFERENCES

1. da Silva, A.M.L., da Costa. Castro, J.F., Billinton, R.: Probabilistic assessment of spinning reserve via cross-entropy method considering renewable sources and transmission restrictions. IEEE Trans. Power Sys. 33(4), 4574–4582 (2017)
2. Clark, C.E., DuPont, B.: Reliability-based design optimization in offshore renewable energy systems. Renewable Sustainable Energy Rev. 97, 390–400 (2018)
3. Muche, T., Pohl, R., Höge, C.: Economically optimal configuration of onshore horizontal axis wind turbines. Renewable Energy 90, 469–480 (2016)
4. Zadeh, L.A.: Fuzzy sets. Inf. Control 8(3), 338–353 (1965)
5. Moradi, M.H., Eskandari, M.: A hybrid method for simultaneous optimization of DG capacity and operational strategy in microgrids considering uncertainty in electricity price forecasting. Renewable Energy 68, 697–714 (2014)
6. Esmaeili, M., Sedighizadeh, M., Esmaili, M.: Multi-objective optimal reconfiguration and DG (distributed generation) power allocation in distribution networks using big bang-big crunch algorithm considering load uncertainty. Energy 103, 86–99 (2016)
7. Alaee, S., Hooshmand, R.A., Hemmati, R.: Stochastic transmission expansion planning incorporating reliability solved using SFLA metaheuristic optimization technique. CSEE J. Power Energy Syst. 2(2), 79–86 (2016)
8. Shafie.Khah, M., Siano, P.: A stochastic home energy management system considering satisfaction cost and response fatigue. IEEE Trans. Ind. Info. 14(2), 629–638 (2017)
9. Reddy, S.S.: Optimal scheduling of thermal-wind-solar power system with storage. Renewable Energy 101, 1357–1368 (2017)
10. Han, X., et al.: Adequacy study of wind farms considering reliability and wake effect of WTGs. 2011 IEEE Power and Energy Society General Meeting, pp. 1–7. IEEE, Piscataway, NJ (2011)
11. Che Yulong, et al.: Probabilistic load flow using improved three point estimate method. International Journal of Electrical Power & Energy Systems 117, 105618 (2020). https://doi.org/10.1016/j.ijepes.2019.105618
12. Choudhary, R., Saket, R.: A critical review on the self-excitation process and steady state analysis of an SEIG driven by wind turbine. Renewable Sustainable Energy Rev. 47, 344–353 (2015)
13. Varshney, L., Saket, R.: Reliability evaluation of SEIG rotor core magnetization with minimum capacitive excitation for unregulated renewable energy applications in remote areas. Ain Shams Eng. J. 5(3), 751–757 (2014)
14. Bansal, R., Zobaa, A.F., Saket, R.: Some issues related to power generation using wind energy conversion systems: an overview. International Journal of Emerging Electric Power Systems 3(2), (2005)
15. Cortez, R.I., Dorrego, J.R.: Analysis of the wake effect in the distribution of wind turbines. IEEE Lat. Am. Trans. 18(04), 668–676 (2020)
16. Abdulrahman, M., Wood, D.: Wind farm layout upgrade optimization. Energies 12(13), 2465 (2019)
17. Ogidi, O.O., Khan, A., Dehnavifard, H.: Deployment of onshore wind turbine generator topologies: Opportunities and challenges. Int. Trans. Electr. Energy Syst. 30(5), e12308 (2020)
18. Khan M.Y., et al.: Placement Optimization for Renewable Energy Sources: Ontology, Tools, and Wake Models. IEEE Access 8, 72781–72800 (2020). https://doi.org/10.1109/access.2020.2984901
19. Zheng, R., Zhou, Y., Zhang, Y.: Optimal preventive maintenance for wind turbines considering the effects of wind speed. Wind Energy 23 (2020). https://doi.org/10.1002/we.2541
20. Grady, S., Hussaini, M., Abdullah, M.M.: Placement of wind turbines using genetic algorithms. Renewable Energy 30(2), 259–270 (2005)
21. Parada, L., et al.: Wind farm layout optimization using a Gaussian-based wake model. Renewable Energy 107, 531–541 (2017)
22. Wilson Dennis, et al.: Evolutionary computation for wind farm layout optimization. Renewable Energy 126, 681–691 (2018). https://doi.org/10.1016/j.renene.2018.03.052
23. Saab, Y.G., Rao, V.B.: Combinatorial optimization by stochastic evolution. IEEE Trans. Comput. Aided Des. Integr. Circuits Syst. 10(4), 525–535 (1991)
24. Beşkirli M., et al.: A new optimization algorithm for solving wind turbine placement problem: Binary artificial algae algorithm. Renewable Energy 121, 301–308 (2018). https://doi.org/10.1016/j.renene.2017.12.087
25. Goldberg, D.E., Holland, J.H.: Genetic algorithms and machine learning. Mach. Learn. 3(2), 95–99 (1988)
26. Kirkpatrick S., Gelatt C. D., Vecchi M. P. Optimization by Simulated Annealing. Science 220(4598), 671–680 (1983). https://doi.org/10.1126/science.220.4598.671
27. Storn, R., Price, K.: Differential evolution–a simple and efficient heuristic for global optimization over continuous spaces. J. Global Optim. 11(4), 341–359 (1997)
28. Colorni, A., et al.: Distributed optimization by ant colonies. Proceedings of the First European Conference on Artificial Life. pp. 134–142.(1992)
29. Deb K., et al.: A fast and elitist multiobjective genetic algorithm: NSGA-II. IEEE Transactions on Evolutionary Computation 6(2), 182–197 (2002). https://doi.org/10.1109/4235.996017
30. Allan R.N., et al.: A reliability test system for educational purposes-basic distribution system data and results. IEEE Transactions on Power Systems 6(2), 813–820 (1991). https://doi.org/10.1109/59.76730
31. Sharifzadeh, M., Lubiano-Walochik, H., Shah, N.: Integrated renewable electricity generation considering uncertainties: The UK roadmap to 50% power generation from wind and solar energies. Renewable Sustainable Energy Rev. 72, 385–398 (2017)
32. Acuña, L.G., Padilla, R.V., Mercado, A.S.: Measuring reliability of hybrid photovoltaic-wind energy systems: A new indicator. Renewable Energy 106, 68–77 (2017)
33. Zitzler, E., Laumanns, M., Thiele, L.: Spea2: Improving the strength pareto evolutionary algorithm. TIK-report 103 (2001)
34. Rodrigues, S., Bauer, P., Bosman, P.A.: Multi-objective optimization of wind farm layouts–complexity, constraint handling and scalability. Renewable Sustainable Energy Rev. 65, 587–609 (2016)
35. Amirinia, G., Mafi, S., Mazaheri, S.: Offshore wind resource assessment of Persian Gulf using uncertainty analysis and GIS. Renewable Energy 113, 915–929 (2017)
36. Srikakulapu, R., Vinatha, U.: Combined approach based on ACO with MTSP for optimal internal electrical system design of large offshore wind farm. 2018 International Conference on Power, Instrumentation, Control and Computing (PICC), pp. 1–6. IEEE, Piscataway, NJ (2018)
37. Jensen, N.O.: A note on Wind Generator Interaction. Risø National Laboratory, Roskilde (1983) https://backend.orbit.dtu.dk/ws/portalfiles/portal/55857682/ris_m_2411.pdf
38. Katic, I., Højstrup, J., Jensen, N.O.: A simple model for cluster efficiency. In: Palz, W., Sesto, E. (eds.) European Wind Energy Association Conference and Exhibition, pp 407–410. A. Raguzzi, Rome (1987)
39. Larsen T.J., et al.: Validation of the dynamic wake meander model for loads and power production in the Egmond aan Zee wind farm. Wind Energy 16(4), 605–624 (2013). https://doi.org/10.1002/we.1563
40. Larsen, G.C.: A simple wake calculation procedure. Risø National Laboratory, Roskilde (1988) https://orbit.dtu.dk/files/55567186/ris_m_2760.pdf
41. Larsen, G.C.: A Simple Stationary Semi-Analytical Wake Model. Risø National Laboratory for Sustainable Energy, Roskilde (2009) https://orbit.dtu.dk/files/122941920/Simple_analytical_wake_model_final_10.pdf
42. Moskalenko, N., Rudion, K., Orths, A.: Study of wake effects for offshore wind farm planning. 2010 Modern Electric Power Systems, September 2010, pp. 1–7. IEEE, Piscataway, NJ (2010)
43. Frandsen, S.: On the wind speed reduction in the center of large clusters of wind turbines. J. Wind Eng. Ind. Aerodyn. 39(1-3), 251–265 (1992)
44. Ott, S., Berg, J., Nielsen, M.: Linearised CFD Models for Wakes. Risø National Laboratory for Sustainable Energy, Roskilde (2011) https://orbit.dtu.dk/files/6354851/ris-r-1772.pdf
45. Sørensen, N.: General purpose flow solver applied to flow over hills. Dissertation, Technical University of Denmark (1995)
46. Wikipedia. Wind rose plot for LaGuardia airport (lga), New York. https://en.wikipedia.org/wiki/Wind_rose (2008). Accessed 14 April 2020
47. Rosenblueth, E.: Point estimates for probability moments. PNAS 72(10), 3812–3814 (1975)

48. Morales, J.M., Perez-Ruiz, J.: Point estimate schemes to solve the probabilistic power flow. IEEE Trans. Power Sys. 22(4), 1594–1601 (2007)
49. Lei, J., et al.: Operation risk assessment of active distribution networks considering probabilistic uncertainties of distributed generators-loads and power management of VRB ESSs. IET Renewable Power Gener. 14(10), 1764–1771 (2020)
50. Che Y., et al.: Probabilistic load flow using improved three point estimate method. International Journal of Electrical Power & Energy Systems 117, 105618 (2020). https://doi.org/10.1016/j.ijepes.2019.105618
51. Naghdalian, S., et al.: Stochastic network-constrained unit commitment to determine flexible ramp reserve for handling wind power and demand uncertainties. IEEE Trans. Ind. Info. 16(7), 4580–4591 (2020)
52. Billinton, R., Allan, R.N.: Reliability Evaluation of Engineering Systems–Concepts and Techniques. Springer US, Plenum Press, New York (1992)
53. Ackermann, T., et al.: Wind Power in Power Systems. John Wiley & Sons, Hoboken, NJ (2005)
54. Bharti, O.P., Saket, R., Nagar, S.: Controller design of DFIG-based wind turbine by using evolutionary soft computational techniques. Eng. Technol. Appl. Sci. Res. 7(3), 1732–1736 (2017)
55. Shakoor, R., et al.: Wind farm layout optimization by using definite point selection and genetic algorithm. 2014 IEEE International Conference on Power and Energy (PECon), pp. 191–195. IEEE, Piscataway, NJ (2014)
56. Ulku, I., Alabas.Uslu, C.: A new mathematical programming approach to wind farm layout problem under multiple wake effects. Renewable Energy 136, 1190–1201 (2019)
57. Kazak, J., van Hoof, J., Szewranski, S.: Challenges in the wind turbines location process in central europe–the use of spatial decision support systems. Renewable Sustainable Energy Rev. 76, 425–433 (2017)
58. Biswal, S.R., Shankar, G.: Simultaneous optimal allocation and sizing of DGs and capacitors in radial distribution systems using SPEA2 considering load uncertainty. IET Gener. Transm. Distrib. 14(3), 494–505 (2020)
59. Moghateli F., et al.: Multi-objective design method for construction of multi-microgrid systems in active distribution networks. IET Smart Grid 3(3), 331–341 (2020). https://doi.org/10.1049/iet-stg.2019.0171
60. Zergane, S., Smaili, A., Masson, C.: Optimization of wind turbine placement in a wind farm using a new pseudo-random number generation method. Renewable Energy 125, 166–171 (2018)
61. Mosetti, G., Poloni, C., Diviacco, B.: Optimization of wind turbine positioning in large windfarms by means of a genetic algorithm. J. Wind Eng. Ind. Aerodyn. 51(1), 105–116 (1994)
62. Turkoglu, B., Kaya, E.: Training multi-layer perceptron with artificial algae algorithm. Eng. Sci. Technol. 23, 1342–1350 (2020)
63. Uymaz, S.A.: Yeni bir biyolojik ilhamlı metasezgisel optimizasyon metodu: Yapay alg algoritması. Selçuk Üniversitesi Fen Bilimleri Enstitüsü, (2015)
64. Beşkirli M., et al.: A new optimization algorithm for solving wind turbine placement problem: Binary artificial algae algorithm. Renewable Energy 121, 301–308 (2018). https://doi.org/10.1016/j.renene.2017.12.087
65. Shakoor R., et al.: Wind farm layout optimization using area dimensions and definite point selection techniques. Renewable Energy 88, 154–163 (2016). https://doi.org/10.1016/j.renene.2015.11.021
66. Pookpunt, S., Ongsakul, W.: Optimal placement of wind turbines within wind farm using binary particle swarm optimization with time-varying acceleration coefficients. Renewable Energy 55, 266–276 (2013)
67. Changshui, Z., Guangdong, H., Jun, W.: A fast algorithm based on the submodular property for optimization of wind turbine positioning. Renewable Energy 36(11), 2951–2958 (2011)
68. Zhang, Y., Gong, C., Li, C.: Surrogate-assisted memetic algorithm with adaptive patience criterion for computationally expensive optimization. 2020 IEEE Congress on Evolutionary Computation (CEC), pp. 1–8. IEEE, Piscataway, NJ (2020)
69. Paul, S., Rather, Z.H.: A new bi-level planning approach to find economic and reliable layout for large-scale wind farm. IEEE Syst. J. 13(3), 3080–3090 (2019)
70. Yang H., et al.: Wind Farm Layout Optimization and Its Application to Power System Reliability Analysis. IEEE Transactions on Power Systems 31(3), 2135–2143 (2016). https://doi.org/10.1109/tpwrs.2015.2452920
71. Kumar S., et al.: Reliability enhancement of electrical power system including impacts of renewable energy sources: a comprehensive review. IET Generation, Transmission & Distribution 14(10), 1799–1815 (2020). https://doi.org/10.1049/iet-gtd.2019.1402
72. Zhao M., Chen Z., Blaabjerg F. Optimisation of electrical system for offshore wind farms via genetic algorithm. IET Renewable Power Generation 3(2), 205 (2009). https://doi.org/10.1049/iet-rpg:20070112
73. Ahmad W., et al.: Formal Reliability Analysis of an Integrated Power Generation System Using Theorem Proving. IEEE Systems Journal 14(4), 4820–4831 (2020). https://doi.org/10.1109/jsyst.2020.2970107
74. Dahmani O., et al.: Optimization and Reliability Evaluation of an Offshore Wind Farm Architecture. IEEE Transactions on Sustainable Energy 8(2), 542–550 (2017). https://doi.org/10.1109/tste.2016.2609283
75. Lingling, H., Yang, F.: Reliability evaluation of the offshore wind farm. 2010 Asia-Pacific Power and Energy Engineering Conference. (2010)
76. Ramli, M.A., Bouchekara, H.R.: Wind farm layout optimization considering obstacles using a binary most valuable player algorithm. IEEE Access 8, 131553–131564 (2020)
77. Subcommittee, P.M.: IEEE reliability test system. IEEE Trans. Power Apparatus Syst. (6), 2047–2054 (1979)
78. Khan Md S.U., et al.: Reliability and economic feasibility analysis of parallel unity power factor rectifier for wind turbine system. IET Renewable Power Generation 14(7), 1184–1192 (2020). https://doi.org/10.1049/iet-rpg.2019.0686
79. Einarsson, S.: Wind turbine reliability modeling. Dissertation, Reykjavik University (2016)
80. Nandigam, M., Dhali, S.K.: Optimal design of an offshore wind farm layout. 2008 International Symposium on Power Electronics, Electrical Drives, Automation and Motion, pp. 1470–1474. IEEE, Piscataway, NJ (2008)
81. Hadidian Moghaddam M.J., et al.: Optimal sizing and energy management of stand-alone hybrid photovoltaic/wind system based on hydrogen storage considering LOEE and LOLE reliability indices using flower pollination algorithm. Renewable Energy 135, 1412–1434 (2019). https://doi.org/10.1016/j.renene.2018.09.078
82. Billinton, R., et al.: Reliability Evaluation of Power Systems. Springer US, New York (1996)
83. Billinton B.R. Evaluation of Different Operating Strategies in Small Stand-Alone Power Systems. IEEE Transactions on Energy Conversion 20(3), 654–660 (2005). https://doi.org/10.1109/tec.2005.847996
84. Fan M., et al.: A Novel Generation Rescheduling Algorithm to Improve Power System Reliability With High Renewable Energy Penetration. IEEE Transactions on Power Systems 33(3), 3349–3357 (2018). https://doi.org/10.1109/tpwrs.2018.2810642
85. Papathanassiou, S.A., Boulaxis, N.G.: Power limitations and energy yield evaluation for wind farms operating in island systems. Renewable Energy 31(4), 457–479 (2006)
86. Kaushal, J., Basak, P.: Power quality control through automated demand side management in microgrid equipped with battery energy storage for protection. IET Gener. Transm. Distrib. 14(12), 2389–2398 (2020)
87. Al.Owaifeer, M., AlMuhaini, M.: Reliability analysis of distribution systems with hybrid renewable energy and demand side management. 2016 13th International Multi-Conference on Systems, Signals & Devices (SSD), pp. 699–704. IEEE, Piscataway, NJ (2016)
88. Jabir, H., et al.: Impact of demand-side management on the reliability of generation systems. Energies 11(8), 2155 (2018)
89. Shafiq S., et al.: Reliability Evaluation of Composite Power Systems: Evaluating the Impact of Full and Plug-in Hybrid Electric Vehicles. IEEE Access 8, 114305–114314 (2020). https://doi.org/10.1109/access.2020.3003369
90. Xu, N., Chung, C.: Reliability evaluation of distribution systems including vehicle-to-home and vehicle-to-grid. IEEE Trans. Power Syst. 31(1), 759–768 (2015)
91. Sultana B., et al.: Review on reliability improvement and power loss reduction in distribution system via network reconfiguration. Renewable and Sustainable Energy Reviews 66, 297–310 (2016). https://doi.org/10.1016/j.rser.2016.08.011

92. Moeini-Aghtaie M., et al.: Generalized Analytical Approach to Assess Reliability of Renewable-Based Energy Hubs. IEEE Transactions on Power Systems 32(1), 368–377 (2017). https://doi.org/10.1109/tpwrs.2016.2549747
93. Wang, T., Zhang, J., Li, S.: Analysis of information reliability on dynamics of connected vehicles. IEEE Access 7, 4487–4495 (2019)
94. Guille, C., Gross, G.: A conceptual framework for the vehicle-to-grid (V2G) implementation. Energy Policy 37(11), 4379–4390 (2009)
95. Clement.Nyns, K., Haesen, E., Driesen, J.: The impact of charging plug-in hybrid electric vehicles on a residential distribution grid. IEEE Trans. Power Syst. 25(1), 371–380 (2009)
96. Dommel, H.W., Tinney, W.F.: Optimal power flow solutions. IEEE Trans. Power Apparatus Syst. PAS-87(10), 1866–1876 (1968)
97. Krause T., et al.: Multiple-Energy Carriers: Modeling of Production, Delivery, and Consumption. Proceedings of the IEEE 99(1), 15–27 (2011). https://doi.org/10.1109/jproc.2010.2083610
98. Tur, M.R.: Reliability assessment of distribution power system when considering energy storage configuration technique. IEEE Access 8, 77962–77971 (2020)
99. Mohamad F., et al.: Development of Energy Storage Systems for Power Network Reliability: A Review. Energies 11(9), 2278 (2018). https://doi.org/10.3390/en11092278
100. Azcarate, C., Mallor, F., Mateo, P.: Tactical and operational management of wind energy systems with storage using a probabilistic forecast of the energy resource. Renewable Energy 102, 445–456 (2017)
101. Abniki, H., Taghvaei, S.M., Mohammadi-Hosseininejad, S.M.: Reliability improvement in smart grid through incorporating energy storage systems in service restoration. Int. Trans. Electr. Energy Syst. 29(1), e2661 (2019)
102. Schweppe, F.C., et al.: A possible future: Deregulation. Spot Pricing of Electricity, In: Schweppe, F. C., Caramanis, M. C., Tabors, R. D., Bohn, R. E. (eds.), pp. 111–128. Springer, Boston, MA (1988)
103. Papathanassiou, S.A., Boulaxis, N.G.: Power limitations and energy yield evaluation for wind farms operating in island systems. Renewable Energy 31(4), 457–479 (2006)

How to cite this article: Kumar S, Saket RK, Dheer DK, Sanjeevikumar P, Holm-Nielsen JB, Blaabjerg F. Layout optimisation algorithms and reliability assessment of wind farm for microgrid integration: A comprehensive review. *IET Renew. Power Gener.* 2021;15:2063–2084.
https://doi.org/10.1049/rpg2.12060